Ice Radar Processor for Prince William Sound – Summary of Configuration and Benefits

R-07-044-546

Prepared for:
Prince William Sound Regional Citizens' Advisory Council

December 2007

Captain Robert A. Bartlett Building
Morrissey Road
St. John's, NL
Canada A1B 3X5

T: (709) 737-8354
F: (709) 737-4706

Info@c-core.ca
www.c-core.ca

This page is intentionally left blank

Ice Radar Processor for Prince William Sound – Summary of Configuration and Benefits

Prepared for:
Prince William Sound Regional Citizens' Advisory Council

Prepared by:
C-CORE

C-CORE Report:
R-07-044-546

December 2007

Innovative Engineering Solutions
Captain Robert A. Bartlett Building
Morrissey Road
St. John's, NL
Canada A1B 3X5

T: (709) 737-8354
F: (709) 737-4706

Info@c-core.ca
www.c-core.ca

The correct citation for this report is:

C-CORE 2007. Ice Radar Processor for Prince William Sound – Summary of Configuration and Benefits, C-CORE Report R-07-044-546 v3.0, December 2007.

Project Team
Desmond Power

REVISION HISTORY

VERSION	NAME	COMPANY	DATE OF CHANGES	COMMENTS
1	Desmond Power	C-CORE	November 6, 2007	First Draft
2	Desmond Power	C-CORE	November 16, 2007	Second Draft
3	Desmond Power	C-CORE	December 21, 2001	Third Draft

DISTRIBUTION LIST

COMPANY	NAME	NUMBER OF COPIES
PWS-RCAC	Joe Banta	1 electronic version

TABLE OF CONTENTS

LIST OF FIGURES

LIST OF TABLES

1 INTRODUCTION

In 2002, under contract from the Prince William Sound Regional Citizens' Advisory Council (PWS-RCAC), C-CORE assisted in the installation of an ice detection radar on Reef Island in PWS (Figure 1-1). The primary function of the ice detection radar is to provide a means to locate icebergs as they calve from Columbia Glacier and drift across the Sound towards the shipping lands. This provides a means for deciding whether it is safe for tankers and other vessels to transect the Sound through the region of highest iceberg density; this region is generally located in front of the Columbia Glacier and in the general vicinity of Point Freemantle and Glacier Island. The installation of the ice radar on Reef Island was a joint initiative, led by RCAC, and involved C-CORE, The US Coast Guard (USCG) and SERVS (Ship Escort/Response Vessel System).

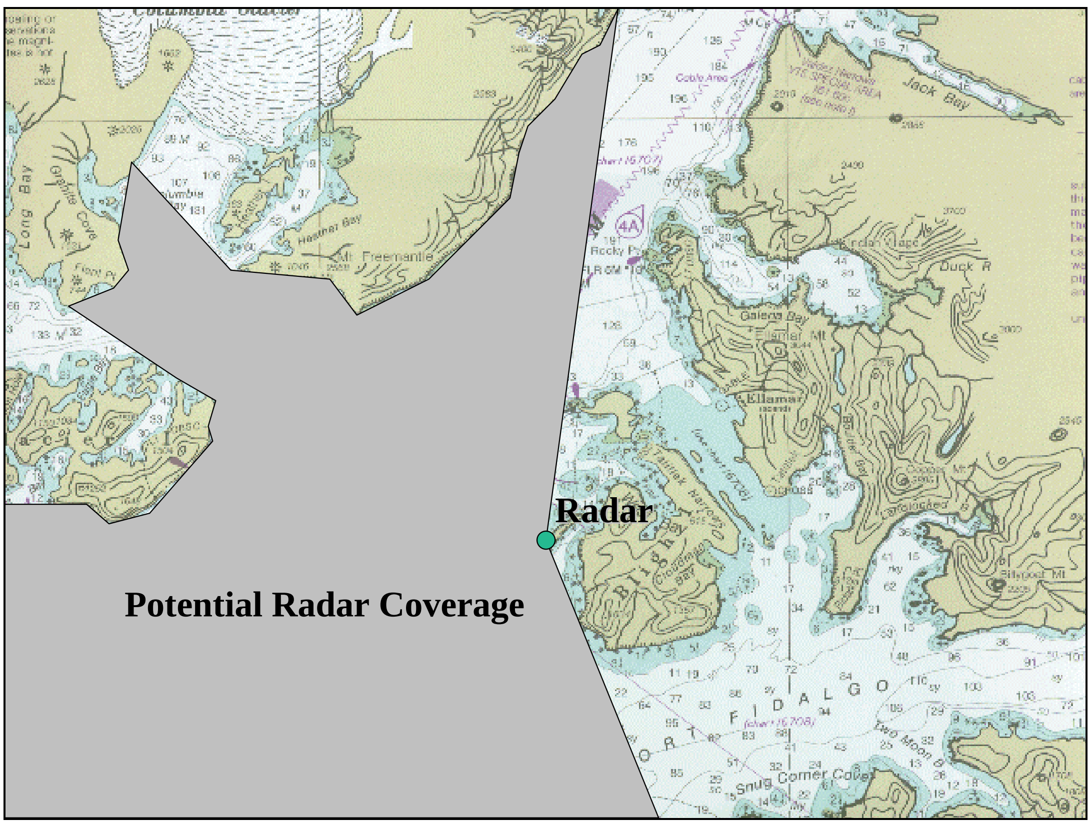

Figure 1-1. Radar coverage from Reef Island radar installation

This report provides a high level overview of the ice detection radar and its functionality. In presenting the details and benefits of the radar system, it is hoped that Reef Island radar system can be maintained in the future for enhanced navigational safety for the Trans-Alaska Pipeline

System (TAPS) operations in the Sound. In addition, there are several features available on the SeaScan that have not been used operationally, and thus recommendations for further use of these features are presented.

The report has been organized as follows:
Chapter 2 provides a general description of the ice detection radar and specialized radar data processor;
Chapter 3 provides an overview of radar detection of icebergs and the details behind the specialized processing used in the Reef Island radar;
Chapter 4 provides an analysis of the latest version Terma radar transceiver (Scanter 2001), and recommendations for installation on Reef Island with the SeaScan processor;
Chapter 5 provides recommendations for future use of the Reef Island radar, including the potential upgrade and modernization of the radar and its data processor; and
Chapter 6 provides a report that was previously prepared by C-CORE (and publicly unavailable until now) on the performance of the SeaScan processor for iceberg detection.

2 REEF ISLAND RADAR DESCRIPTION

The ice detection radar is physically located on Reef Island (Figure 2-1), a site which was deemed to have a superior field of view of the Valdez shipping lanes and the icebergs calving from the Columbia Glacier. While there are two other radar sites in the Valdez Region (Potato Point and Valdez Spit) operated by USCG, neither of these two sites provide a direct view of the icebergs as they approach the traffic lanes from the Glacier. The Potato Point site does have a view of the traffic lanes out through Valdez Arm; however, the view is limited to the traffic lanes themselves and not to the surrounding areas from which the icebergs drift. On the other hand, the Reef Island site has a view of traffic lanes and the source of the icebergs from the Glacier. The Reef Island site also has a significant elevation advantage over Potato Point; thus Reef Island provides a much greater probability of iceberg detection.

Figure 2-1. Reef Island radar site showing SERVS equipment shelter, microwave communications tower (left) and radar tower (right)

2.1 Radar Equipment

The ice detection radar includes an X-Band Terma radar (9.3-9.5 GHz transceiver and 18 foot antenna) and a radar data processor known as the SeaScan processor[1]. The Terma radar was supplied in-kind as a contribution to the ice radar project by the USCG. RCAC supplied funding to install the radar tower upon which the radar antenna is installed and the radar equipment (Terma transceiver and SeaScan) is installed in an equipment shelter that is owned and maintained by SERVS. The data feed from the radar is transmitted from Reef Island to Valdez via a microwave link maintained and operated by SERVS. A high level block diagram of the ice radar is shown in Figure 2-2.

[1] The SeaScan processor is now sold under the trade name Sigma S6 Ice Navigator by Rutter Inc.

Note that the block diagram below shows that the Terma radar is connected to the Seascan processor and a second unit called the Lockheed Martin IAU/RDP via the standard radar interfaces. The Lockheed Martin (LM) unit is a radar data processor (RDP) that provides a radar signal back to USCG; the LM-RDP is a similar data processor to the ones installed at the Potato Point and Spit site radars, and thus the data feed is of similar quality and format for the USCG's standard radar displays. Further details of the SeaScan processor, and a comparison to the LM-RDP, are provided in the sections that follow.

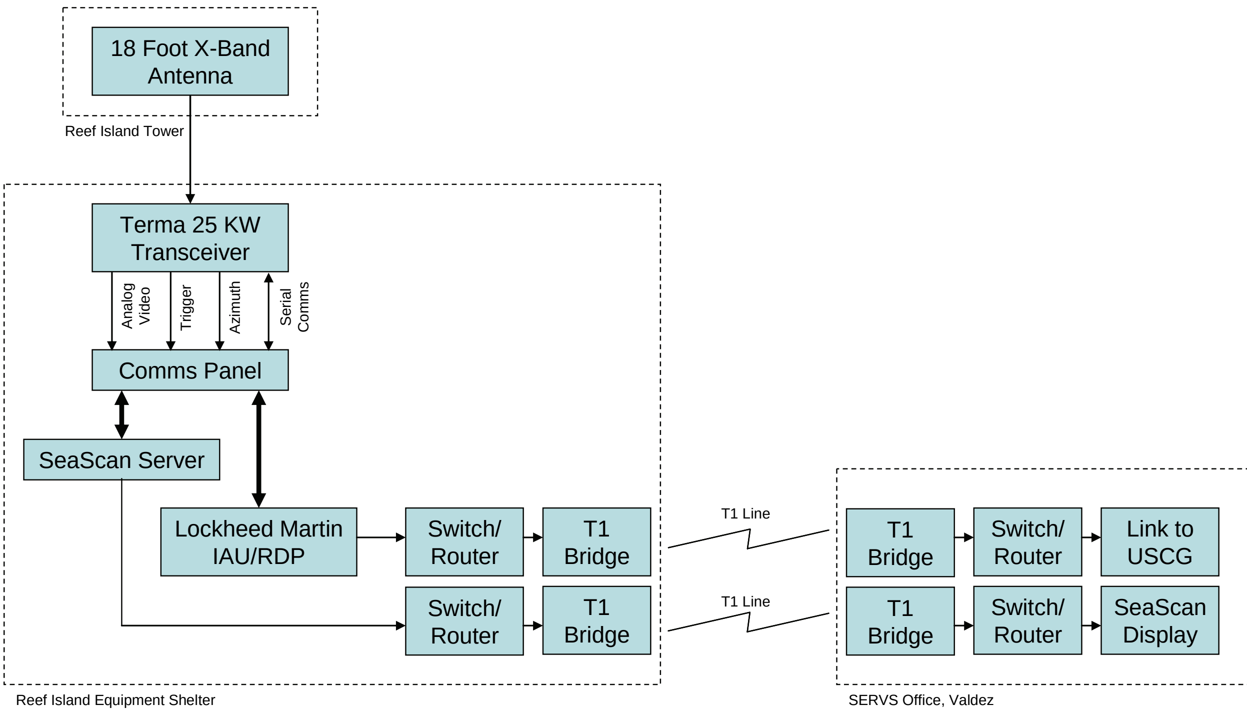

Figure 2-2. Ice Detection Radar at Reef Island

2.2 SeaScan Processor Details

The SeaScan is a radar data processor that provides various enhancements to normal radar signals. The SeaScan is not a complete radar unit, but rather is a radar data processing computer; as such, it requires a radar transceiver and antenna to operate properly. In the case of the Reef Island site, the radar unit coupled to the SeaScan is the Terma radar as shown in Figure 2-2. The figure shows two SeaScan units, including a radar data processor/server at Reef Island and a radar display that is installed in the SERVS duty office. A playback unit was also provided as part of the complete SeaScan package to be used as a radar training unit.

2.2.1 SeaScan Data Processor/Server

The SeaScan data processor, pictured in Figure 2-3, is a computer that serves as both a processor and server. The processor portion of the computer takes the analog radar video feed from the Terma Radar and digitizes it at 12 bit resolution for further signal processing. The unit has a variety of standard software selectable radar processing functions including:

- Pulse-to-pulse filtering;
- Scan-to-scan averaging;
- CFAR (constant false alarm radar) target detection;
- Scan conversion;
- Plot extraction; and
- Target tracking.

Figure 2-3. SeaScan radar data processor and server

The data server functionality of the SeaScan allows the unit to store raw radar data to tape for later playback and training. The SeaScan records digitized raw video to tape (along with ancillary data) which is a complete radar picture with a refresh rate of ~3 Hz. Since the full bandwidth radar signal cannot be transmitted over the limited communications bandwidth that exists between Reef Island and SERVS, the recording operation can ONLY be accomplished at Reef Island. To get the radar signal back to Valdez, the data server relays a *processed* radar signal back to SERVS via the microwave communication link. Since the available data bandwidth on this microwave link does not allow for a full bandwidth signal, the SeaScan processor reduces the refresh rate of the radar display to match the available bandwidth. The result is a radar update rate of approximately once per minute. By reducing the refresh radar of the radar signal, the dynamic range of the radar picture is preserved allowing for good imaging of icebergs. This is the fundamental difference between the SeaScan processor and the LM-RDP. Since the USCG requires its radar for vessel traffic management, the refresh rate of their radar display has to mirror that of the radar antenna speeds (i.e., ~2.5 Hz). Since the data bandwidth of the microwave link does not support transmission of the full resolution radar signal, the LM-RDP converts the radar signal into a 'detected product' with a reduced dynamic range. The 'detect product' has been tuned by LM to meet the needs of vessel traffic management, which is mainly ship detection. Since iceberg radar returns are much reduced compared with vessels, many icebergs will not be detected by the LM-RDP. In addition, the LM-RDP does not include scan-average processing, which provides a significant enhancement for slow moving iceberg targets. Complete details of this are provided in the next chapter of this report.

2.2.2 SeaScan Display

To display data from the SeaScan processor, a plan position indicator (PPI), which is the most common type of radar display, is provided as a software application. In a PPI display, the radar antenna is usually represented in the center of the display, so the distance from it can be drawn as concentric circles. As the radar antenna rotates, a radial trace on the PPI sweeps in unison with it about the center point. Due to the reduced bandwidth microwave communications from Reef Island, the SeaScan PPI is only updated about once a minute, rather than as the radar antenna rotates. A picture of the SeaScan display is provided below in Figure 2-4. This display does not include any radar processing capabilities, but simply displays the radar feed that is emanating from the SeaScan processor/server at Reef Island.

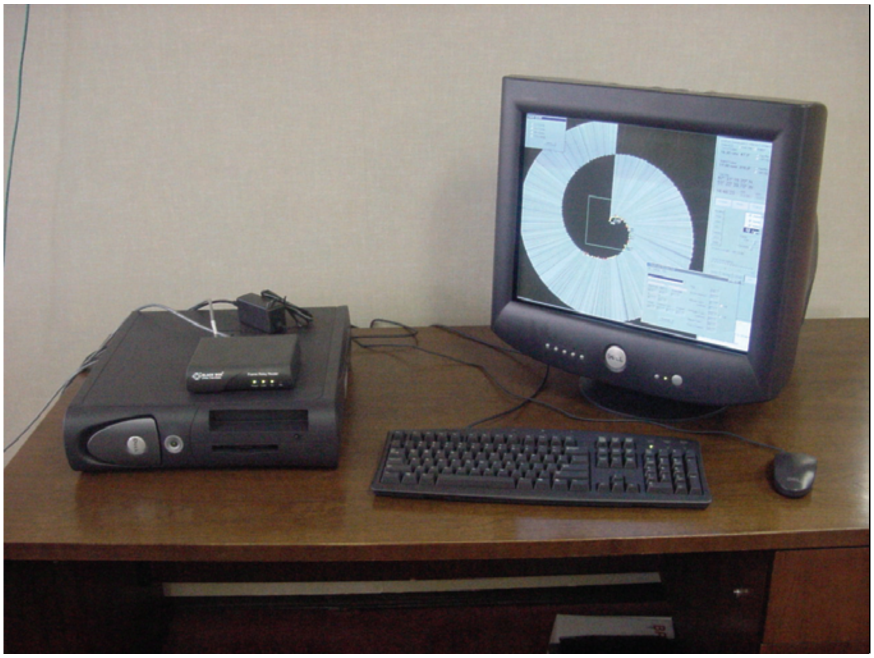

Figure 2-4. SeaScan radar display (presently installed at the SERVS duty office)

In addition to providing a radar display, the SeaScan software also includes functionality to control the radar and data processing functions. In this configuration, commends are sent from the display to the SeaScan processing unit at Reef Island, which in turn sends control signals to the Terma transceiver unit. Since it was deemed appropriate that the Terma radar functions be controlled by USCG, the radar remote control functions of the SeaScan display have been disabled. Instead, the main functionality of the SeaScan display software is to control the 'radar processing functions' of the Reef Island SeaScan processor, including scan-to-scan averaging, pulse filtering and CFAR.

In its current configuration, the SeaScan radar feed can by made available to several displays at one. The main display at the SERVS duty office can be replicated via the internet to other SeaScan terminals. These secondary SeaScan terminals do not require a direct connection to the SeaScan processor on Reef Island, but rather have the display information on the SERVS duty office computer 'duplicated' in other locations. This would require that the SERVS duty office SeaScan display be able to communicate via the internet to the other remote locations (such as at USCG or RCAC offices)

2.2.3 SeaScan Playback Unit

The SeaScan processor was supplied with data recording capabilities. This allows for recoding the full bandwidth radar signal from the Terma radar at Reef Island to an Exabyte tape for later playback. This allows for offline training of personnel in the use of the SeaScan and its functionality. The playback of radar data can be accomplished on the Reef Island SeaScan processor, or on a separate Playback Unit that was supplied to RCAC and installed at the Prince William Sound Community College. A picture of the SeaScan playback unit is provided in Figure 2-5. The playback unit has all of the software functionality of the Reef Island SeaScan processor, including scan-to-scan averaging, pulse filtering and CFAR. Since the radar data is stored on tape in raw format, the playback unit can process the data in a variety of different manners (e.g., turning scan-averaging off and on) and can be used to process the same data over and over again. Thus, it is an ideal tool for training. Since the SeaScan playback unit is a regular PPI display, it can be used for training personnel on the use of standard radars, and not just those functions that are specific to the SeaScan.

Figure 2-5. SeaScan playback unit (presently installed at PWS Community College)

3 ICEBERG MONITORING WITH RADAR

When monitoring for icebergs, whether it be via satellite, aircraft or vessel, the most important sensors are radar-based. Regions frequented by ice can generally be characterized by considerable fog, cloud, and precipitation, which can preclude effective visual detection. This leaves radar-based systems as the primary surveillance tool. Radar was invented for the primary purpose of wide area surveillance for encroaching targets such as vessels or aircraft. The fact that icebergs and sea-ice can also be detected by radar is an added benefit, making these sensors multipurpose. However, ice is a much different target in both composition and expected movement than other radar targets, and many studies have been conducted to enhance the detection of ice in the conditions under which ice persists. A short list of studies include those by C-CORE (2000-2005), Crocker et al. (1998), Haykin et al. (1994), Harvey and Ryan (1986), Howell et al. (2007), Kline et al. (1986), McClintock et al. (2007), Robe et al. (1985), Rossiter et al. (1985), and Ryan et al. (1985). These studies generally conclude that radar can be used effectively for iceberg detection, however there are specific modes under which radars can operate to enhance probability of detection.

The following section provides some additional detail on the factors that affect iceberg detection. This is followed by a description of the techniques that can be used specifically with terrestrial-based radar to maximize iceberg detection for surveillance purposes.

3.1 Factors that Affect Radar Iceberg Detection

Regardless of the radar type, detection of icebergs is dependent on several factors, including iceberg size, electromagnetic reflectivity, meteorological conditions and sensor parameters. The following sections list the parameters that must be considered when analyzing radar performance.

3.1.1 Iceberg Radar Cross Section

Icebergs are composed of glacial ice of freshwater origin, and this composition generally limits the detectability of icebergs relative to other ocean targets, such as vessels or ocean backscatter (sea clutter). The extent to which an object reflects an incident electromagnetic wave from a radar system is usually characterized in terms of a Radar Cross Section (RCS). The RCS is a measure of the strength of the radar signal backscattered from a "target" object for a given incident wave power.

Several studies on the response of icebergs to radar energy have been conducted (Haykin et al., 1994, Ryan et al. 1985, Rossiter et al., 1985, Harvey et al. 1986, Robe et al. 1985). Most have concluded the following key points:

- Glacial ice found off Newfoundland has a reflection coefficient that is much lower than that of the materials found in vessels, and consequently icebergs reflect radar waves at a much lower intensity. This is highly dependent on radar frequency, iceberg shape and size; however, on average icebergs have a RCS that is between 10 to 100 times (10 to 20 dB) less than an equivalently sized ship.
- The reflectivity of glacial ice found in icebergs is highly frequency dependent, and generally the iceberg RCS increases with increasing frequency. In the case of icebergs, the reflectivity (RCS) is higher at X-Band (9.3-9.5 GHz) than S-Band (3 GHz).

Despite the lower reflectivity of icebergs, they are nonetheless detectable with radar, albeit with a lower probability of detection than equivalently sized vessel targets.

3.1.2 Environmental Conditions

Environmental factors such as wave height, wind speed, and precipitation affect the performance of various radar systems to varying degrees. These factors serve to directly obscure targets (in the case of sea swell), to produce unwanted radar clutter (i.e., unwanted radar echoes) and to attenuate the radar signal.

Sea clutter is perhaps the most limiting environmental factor for target detection on the ocean, and is produced by ocean waves that are resonant with the radar wavelength. At microwave frequencies, the radar wavelengths are resonant with capillary waves, those small ocean waves that are quickly generated as the wind increases. As such, ocean clutter levels in microwave radars are well correlated to wind speed. The intensity of sea clutter generally increases with increasing frequency; this is why S-Band marine radar (3 GHz) typically outperforms X-Band radar (9.3-9.5 GHz) when the wind speeds are high even though the reflectivity of icebergs is higher at X-Band than at S-band.

Rain is also a factor of consideration with X-Band radar since rain produces both clutter and signal attenuation. On the other hand, S-Band radar is generally not susceptible to either rain clutter or attenuation. Most standard marine radars come equipped with a radar antenna that is horizontally polarized, which means that the antenna transmits and receives microwave radiation that oscillates in a plane parallel to the earth's surface. This is standard practice with marine radar because vertically polarized radiation produces more sea clutter than horizontally polarized radiation. The Terma radar is equipped with a circularly polarized antenna array; circular polarization provides lower susceptibility to precipitation and sea spray as the shape of individual water drops approaches that of perfect spheres. A perfect sphere reverses the rotation of a circularly polarized wave and thus the backscatter from a spherical rain droplet will be a reverse polarization to other types of backscatter (e.g., from ships or icebergs). Since the receiving antenna is tuned to received radiation that is polarized in one direction only, backscatter from rain is suppressed. This dramatically reduces the effects of rain clutter, although the effects of rain attenuation are still present that might reduce the radar echoes of other targets.

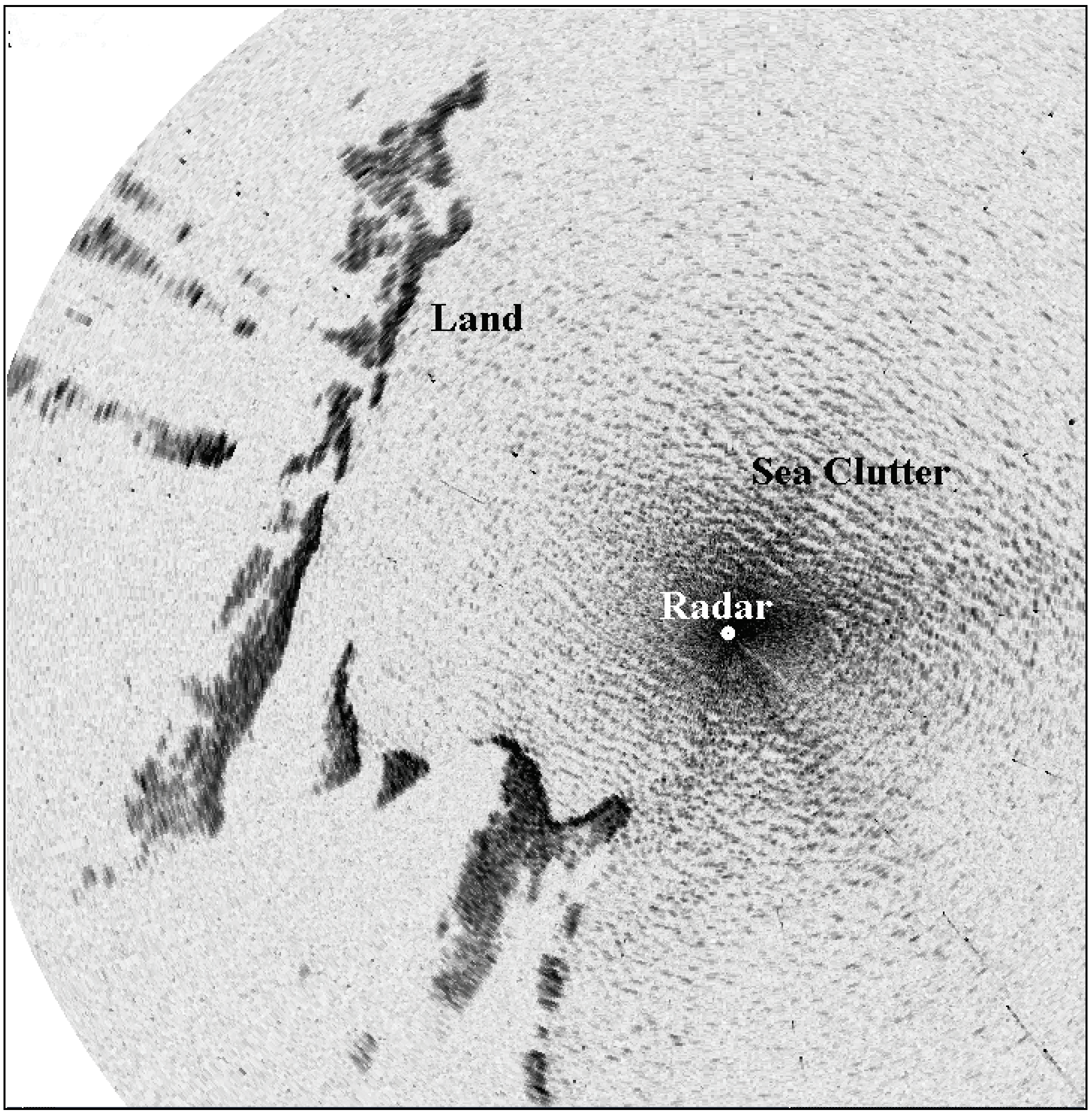

Figure 3-1. Terrestrial microwave radar data showing sea clutter

3.1.3 Grazing Angle and Incidence Angle

For terrestrial based radar, the grazing or depression angle is the angle of the direction of radar waves relative to the ocean surface. This grazing angle will be dependent on the height of the radar antenna and on the range of the ocean surface as shown in Figure 3-2. Near ranges will have larger grazing angles (ϑ_1 in Figure 3-2) than far ranges (ϑ_2 in Figure 3-2).

The term angle of incidence is also used to describe the location of the radar relative to a location on the ground. Incidence angle is usually the term used in satellite or aerial radar due to the fact that the attitude of the radar is generally on the order of the range to the target. The incidence angle is the angle between the radar's line of sight and a normal (i.e., 90°) to the ground (θ in Figure 3-2). Thus, the incidence angle and grazing angle are related as $\theta = 90 - \tilde{\vartheta}$. Thus, near ranges have small (or steep) incidence angles while far ranges have large (or shallow) incidence angles.

Generally, ocean clutter increases with grazing angle because the ocean surface is physically a larger target at higher grazing angles. This target is the projected area of the ocean surface on a plane perpendicular to the direction of radar signal, which decreases with decreasing grazing angle. As such, an increase in the grazing angle (or a decrease in the incidence angle) will generally produce higher clutter returns at the same radar range.

The grazing angle can also affect the RCS of targets, such as icebergs or ships. This is due to the underlying geometry of the target scattering, which may result in stronger or weaker echoes depending on how the target is oriented relative to the radar. While no systematic studies have been done on this with icebergs, recent work by C-CORE using satellite based C-Band (5.4 GHz) synthetic aperture radar (SAR) data shows the incidence angle dependence of iceberg RCS. As shown in Figure 3-3, shallow and steep incidence angle seems to produce the highest icebergs radar cross sections, with a minimum occurring at ~53°. Since large incidence angles also produce the lowest clutter conditions, it is reasonable to assume that the highest probability of detection will occur at these conditions, except in the case of terrestrial radar where the horizon limit has been exceeded (see further, next section).

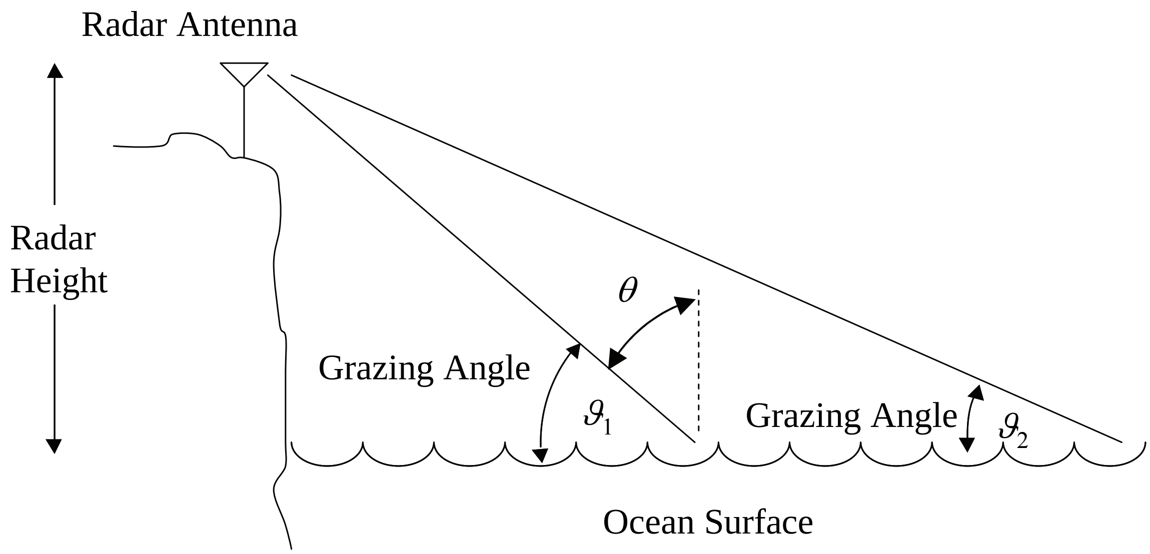

Figure 3-2. Radar grazing angle

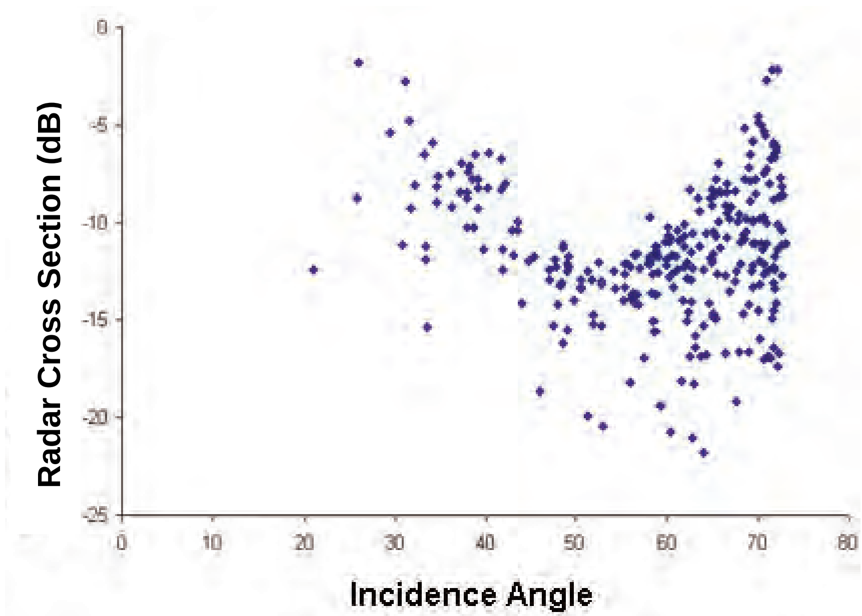

Figure 3-3. Incidence angle dependence on iceberg RCS (C-Band)

3.1.4 Radar Height

The height of a radar sensor affects the performance of the radar in two ways, specifically the received ocean clutter and maximum range. As discussed in the previous section, steeper incidence angles are subject to increased ocean clutter, thus the higher the radar's antenna, the more clutter will be produced in the near ranges of the radar.

Conversely, the maximum radar range will increase with increasing radar height. All terrestrial radars (with the exception of those that operate below 50 MHz) are line of sight sensors, meaning they can only "see" as far as the horizon. The radar horizon is directly related to the radar height as per the formula $4128\sqrt{h_a}$, where h_a is the height of the radar's antenna. Thus a vessel with its radar antenna height of 30m will have a maximum radar range of 22.6 km, while an offshore oil rig, with the antenna atop the derrick at 76m, will have a maximum range of 36 km. The radar 'horizon' equation is equally applicable to aerial radar as it is to terrestrial radar. However, for satellite radar, the horizon range limitation is not a consideration because the orbits are on the order of hundreds of kilometers. Instead, the satellite radars have fixed 'swath widths' with maximum incidence angle of <70°.

3.2 Terrestrial Microwave Radar

3.2.1 Traditional Radar

Marine radar is a term usually used to describe a class of microwave radars that have been approved for use on vessels by the International Maritime Organization. They are generally available in two frequency bands (S and X) corresponding to the two IMO approved bands for this application. They operate using a rotating transmit and receive antenna (scanner) coupled with a standard PPI display.

Marine radar, in its various derivatives, has been the staple of iceberg detection since its invention in the 1940's. Most of the early ice surveillance conducted from drill ships relied solely on the vessels 9 kW, X-Band marine radar for iceberg detection. These units provided typical detection distances of 10 nautical miles for small icebergs, which proved suitable for the type of management conducted at the time.

Today, there are various configurations of marine radar offered by various companies and approved for use by the IMO under the SOLAS (Safety of Life at Sea) Convention. Typical power levels of these radars are on the order of 25-30 kW peak, with antenna sizes of up to 4 metres long.

High end surveillance radars are also available with higher power levels and antenna sizes than marine radar. These class of radars are not IMO approved for use on vessels since they are typically deployed terrestrially for VTS (Vessel Traffic Service) applications or air traffic control. The Terma radar used in the Reef Island system is one such example of a high-end surveillance radar. This class of surveillance radar typically has a number of special processing features for small target detection built into their radar data processing (RDP) units. Alternately, third party RDPs can be purchased as an add on to existing surveillance or marine microwave radar; The SeaScan processing is an example of this type of RDP. Since high-end surveillance radars have higher power levels, larger antennas and enhanced data processing capabilities, the probability of iceberg detection is significantly enhanced using these radars compared with traditional marine radar.

The higher frequency X-Band radar will provide slightly better performance in benign conditions over the S-band radar for two reasons; the X-band antenna will provide a higher azimuthal resolution over an equivalently sized S-band antenna, and iceberg targets have a higher radar cross section at X-Band compared to S-Band (Harvey and Ryan, 1986, Ryan et al., 1985). Conversely, S-Band radar will have better performance in high clutter conditions (i.e., high winds and sea-state) and adverse weather (Rossiter et al., 1995). To achieve the highest performance in all conditions, vessels that operate in ice frequented waters are recommended to have radars at both S and X-Band mounted at the highest available vantage point to achieve the best horizon limit. This configuration has been shown to provide the best detection capability over single frequency systems (Ryan et al., 1985).

3.2.2 Enhanced Microwave Radar

Since the mid 1990's, advanced *after-processors* (i.e., RDPs) have been available for microwave radars. In the case of high-end surveillance radars, an RDP unit may come built in to the units themselves. However, in the case of traditional marine radar, RDPs can be purchased as an add-on. These third-party *after processors* digitize the raw radar video signal (the signal that is routed to the PPI) and performs advanced signal processing, such as CFAR, pulse filtering and scan integration. The benefits of having a RDP that is *external* to the radar is that it allows the installation of two different PPI displays, one specifically on vessel traffic management and general navigation and one for iceberg detection. The use of two displays is necessary in vessel traffic management applications because the enhancement of the radar signal for iceberg detection can smear fast moving targets, thus making it unsuitable as a VTS display. A second display and processor also allows for independently setting target detection criteria, which allows for the ice radar display to be tuned specifically for icebergs and sea-ice.

One particular processor, the SeaScan from Rutter Technologies, has been extensively tested for iceberg detection and it has been proven to be highly effective at enhancing the signatures of iceberg targets. RDP units that have similar capabilities to the SeaScan can be expected to perform similarly for enhanced iceberg detection.

Icebergs are generally slow moving targets with a low RCS, and as such, scan integration is highly effective at enhancing their target signatures in the presence of sea clutter. Scan integration, also known as incoherent averaging, is a means over averaging a number of radar scans together. The overall effect is to smooth and reduce sea clutter and noise while enhancing slow moving or stationary targets. An example of this effect is shown in Figure 3-4 which shows an array of small buoys that are undetectable in the unprocessed radar signal but are easily seen in the scan-averaged data. The target enhancement is limited by several factors including the relative motion of the target of interest to the radar and the limit to which clutter is reduced by incoherent averaging. To achieve maximum effect on a moving platform such as vessel or FPSO, motion compensation by means of an inertial navigation unit may be necessary. Note that the buoy targets shown in the figure below are stationary and the enhancement of the buoy targets are reliant on the fact that target returns from the buoys overlay one another and are *additive*. In the case of a moving vessel target, the radar signature on a scan-averaged display would manifest itself as a streak across the display. Icebergs tend to be very slow moving and are *more or less* stationary over the integration time of the scan-average processing. Thus, these targets are enhanced through successive radar scans.

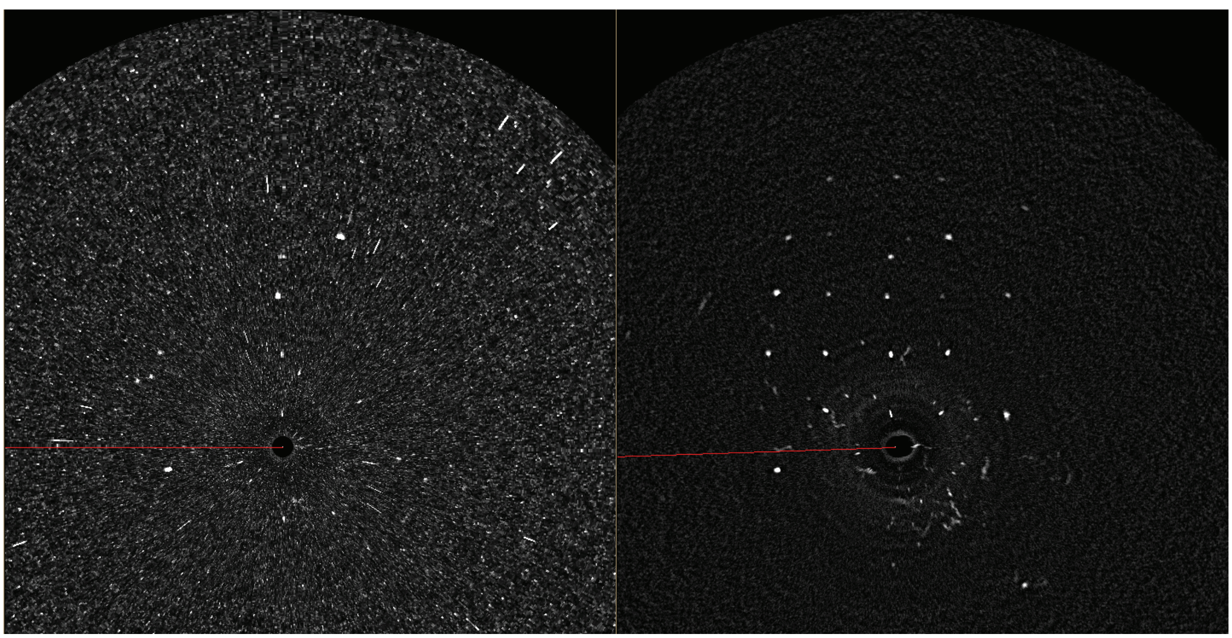

Figure 3-4. Advanced after-processor for marine radar (SeaScan) – (left) Raw radar return, (right) Reduced clutter through scan-to-scan processor (24 scans)

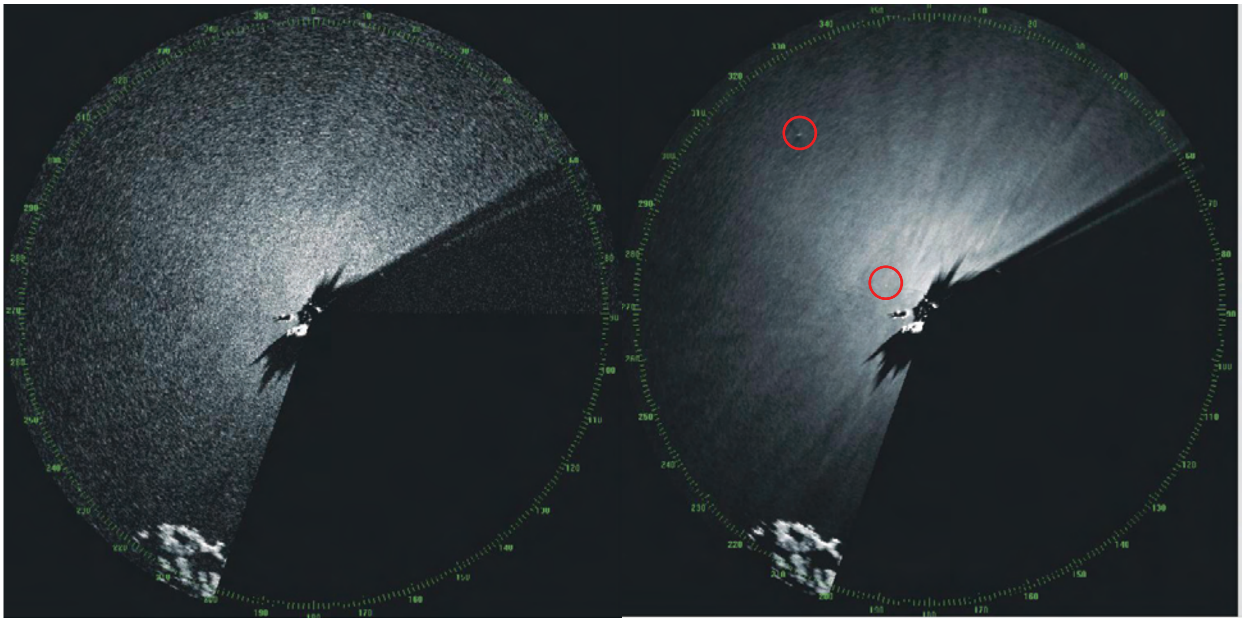

Figure 3-5. Scan integration for iceberg detection – (left) Raw radar return, (right) Reduced clutter through scan-to-scan processor (24 scans) that reveals two iceberg (growler) detections.

C-CORE, through its Integrated Ice Management R&D Program (IIMI), performed extensive testing on the SeaScan processor for iceberg detection in 2001 (C-CORE, 2002) using a Raytheon Pathfinder X-Band marine radar with a 25 kW transmitter and a 7 foot antenna. While this configuration is not the optimal available for iceberg detection (see previous section), reliable detection of small icebergs was consistently achieved out to 60 km for small icebergs and to 35 km for bergy bits. Examples of data processed by the SeaScan processor are provided in Figure 3-5. The complete report for this 2001 field program, previously unavailable to the public, has been declassified and have been included as Chapter 6 of this report.

It is important to note here that, for the radar to display icebergs targets at the highest level of enhancement, the dynamic range of the display (in terms of grey-levels and contrast) is much different than a traditional PPI display used in vessel navigation or a VTS. Traditional displays generally limit the dynamic range to as little as two levels (i.e., detected or not). For weak iceberg targets, this is definitely not the optimal choice of display since there is a significant amount of information that is lost in such a display that could easily be interpreted by a radar operator. It is also important to note that a radar operator will need additional training in the use and interpretation of such a high dynamic range display. Normally, a radar operator would not receive training in the interpretation of ice in radar imagery from a traditional radar training course.

3.2.3 Coherent Microwave Radar

Traditional microwave radars, such as the Terma, use magnatrons to generate their microwave pulses. These devices are very effective at producing short intense bursts of microwave power, and the radars rely on the narrow-in-time pulses to provide good resolution in the range direction. The limitation of a magnetron is that the pulses are not well controlled in frequency, and thus a tuner must be used on the radar receiver to track the transmitted frequency. As such, there is a limitation that can be achieved in averaging pulses together to enhance the radar returns, as discussed in the previous section on *Enhanced Microwave Radar*. With modern communications systems encroaching on the traditional S-Band radar frequency allocation, there is ongoing international pressure to 'clean up' the microwave radar spectrum. This is the rationale behind recent efforts to produce commercial 'coherent' microwave radars.

Coherent Radars are radars that use waveform design and pulse control to emit a controlled burst of energy. This type of radar has been available in more expensive military, aerial and satellite based radar and has only recently become popular due to advances in microwave telecommunication equipment. Coherent radars typically use solid state transmitted to produce 'clean' power transmissions. While these type of transmitters produce power levels that are much lower than magnetrons (on a cost per kilowatt basis), pulse compression can be used to produce transmissions that are equivalent to the power level produced by a traditional marine radar. Pulse compression works by transmitting a pulse that is longer in duration than a typical radar pulse. Since time translates into distance in a radar system, traditional radars have *short* pulses to provide for adequate range resolution. As a consequence, the short pulses have to be very intense so that an adequate amount of energy is imparted on the target. However, if a *coded* pulse is used instead, signal processing (pulse compression) can be imparted to *compress* a long pulse in time to be equivalent to a short pulse. Thus, a radar that includes pulse compression can transmit longer pulses that are less intense, but still impart the same amount of energy on a target and achieve a similar range resolution. Pulses are either coded by frequency or phase modulation, which can easily be achieved using a solid state transmitter, but not with a magnetron.

The IMO has recently approved a Coherent S-Band standard, which is expected to replace traditional marine microwave radar at S-Band in the next decade. C-CORE, in several programs funded by the IIMI and the Canadian Coast Guard, have developed coherent S-band prototype that has been tested for iceberg detection through the IIMI program (C-CORE, 2000, 2003). This prototype is expected to reach commercial maturity by 2009. Other radar companies, including JRC and Kelvin-Hughs are marketing coherent radars that presently meet the IMO standard. While the IMO standard has been released, this technology is presently in its infancy.

Significant improvements of this technology are expected over the next five to 10 years. This technology is well suited to improved detection due to the processing gains that can be achieved with the coded transmissions.

4 EVALUATION OF THE NEW TERMA RADAR

The USCG has procured two new Terma radars for the Potato Point and Spit site radar stations. The radars include a Scanter 2001 X-Band transceiver and a 21' high gain X-band antenna. The new transceiver is said to be an upgrade from the existing Terma transceiver. This section of the report suggests recommendations for a potential future deployment of this radar to the Reef Island site and the recommended configuration of the radar with the existing SeaScan processor.

4.1 Features and Advantages of New Terma Radar

Rather than make a direct comparison of the old Terma transceiver that exists at Reef Island to the new Scanter 2001, a set of high level observations will be made on the specifications of the new Scanter 2001, which were made available to RCAC for preparation of this report.

The first observation that is notable about the new Terma radar is the size of the antenna. The new system includes a 21' antenna, which is three feet longer than the existing 18' Reef Island antenna. The larger antenna will provide for enhanced target detection and reduced clutter just by the fact that the gain is higher and the azimuth beam width is narrower. It is expected that icebergs would be more easily detected and discriminated with this upgraded antenna system.

The second observation that is made is on the level of data processing that exists with the Terma's internal RDP. The new transceiver includes the following enhanced surveillance features that are normally not included in a standard marine radar package (but are available in all new Terma transceivers).

- Frequency diversity – this feature is also available on the existing Reef Island Terma transceiver. It allows for enhanced target detection and reduced clutter through the incoherent averaging of radar pulses of two different frequencies.
- Video processor – the Terma transceiver performs 8-bit analog to digital conversion of radar data stream to a form that can be manipulated by digital signal processing. The video processing works in conjunction with the frequency diversity feature of the transceiver and includes a noise cancellation circuit. The output of the video processor includes both analog video and digital video (with frequency diversity enhancements).
- Auto-sensitivity control – this feature is described as a means to adapt to varying levels of sea-clutter by auto-compensating small windows of data to varying clutter levels. The way this processing is described, it is interpreted as a standard CFAR algorithm, such as the one that exists on the SeaScan processor.
- Sea-Clutter discriminator – this feature uses scan-to-scan averaging in three parallel channels, which are subsequently combined. The three parallel channels have different

levels of scan-to-scan averaging combined with a varying detection threshold for various target types. The first channel is for very slow targets (up to 8 knots) and includes a very low detection threshold and three consecutive scans averaged. The second channel is for moderate speed targets (up to 16 knots) and includes a low detection threshold and two consecutive scans averaged. The third channel is for fast moving targets, and as such does not include any scan-to-scan averaging and a normal detection threshold. Signals from the three channels are combined giving the operator and tracking system a combined picture from all three channels.

4.2 Interfacing/Comparison of SeaScan Processor and Terma Radar

It is noted from the Scanter 2001 specifications that analog video is provided as a standard output, along with trigger and azimuth data in an industry standard format. Therefore, it appears that the SeaScan processor in its current configuration can be easily interfaced to the Scanter 2001 without significant modifications.

Concerning the analog video outputs, it is stated in the Scanter 2001 specifications that the Video Processor performs 8-bit analog to digital conversion before frequency diversity processing. The SeaScan's video processor has a 12-bit analog to digital converter which is a much higher dynamic range than the Terma's 8-bit converter. The higher dynamic range has been shown to be an enhancement to detecting and discriminating ice, which has a much weaker target signature than vessels, as stated in section 3.1.1. Thus, the additional dynamic range of the SeaScan over the Terma is a considerable advantage in imaging ice. Since the analog video outputs (up to four in total) can be software configured, it is recommended that one of these video outputs be configured to bypass the Terma video processing unit (which performs the 8-bit analog to digital conversion) which could degrade iceberg detection performance. Although this would also bypass the frequency diversity processor, the advantage of the additional dynamic range offered by the SeaScan is a much higher priority for iceberg detection.

The Terma radar includes scan-to-scan averaging, which gives a significant advantage over standard marine radars for imaging ice. However, the maximum number of scans that can be processed is limited to three. On the other hand, the SeaScan processor, in its current configuration, can process up to 128 scans. The scan averaging processing is deemed to be the most important enhancement for iceberg detection. Combined with the 12-bit video conversion, the addition of the SeaScan processor with the Terma radar is considered to be a significant advantage for mapping icebergs compared with the Terma radar alone.

4.3 Expected Performance of New and Existing Radars

The performance of the Reef Island ice detection radar can best be illustrated by a representative example. In this case, the example used is the probability of detection of a bergy bit of length 12 metres in relatively rough ocean conditions (6 ft swell and 18 knots wind speed). Iceberg detection can be most problematic in these types of conditions with standard radar systems. A radar model was used to plot the detection performance; the radar model used in this case was the model that was validated in the 2001 field program, conducted by C-CORE (see further Appendix A to this report).

The performance is best illustrated be comparing a stand-alone Terma radar with a Terma radar and SeaScan processor combination. Given that the Potato Point and Spit site radars will be upgraded with new Scanter 2001 and 21' antenna, a comparison is also made between the old Terma system and the new Scanter 2001. The following configurations have been modeled:

1. Existing Terma Radar: The radar that currently exists at Reef Island (18' antenna) was used in the first simulation. The first simulation was performed with no scan averaging (i.e., no SeaScan) and thus the results mimic the performance achieved with the radar display that currently exists at the USCG for the Reef Island radar.
2. Existing Terma Radar with SeaScan: This configuration is identical to (1) above, except the SeaScan processor has been added. The simulation has been performed with 16 scans, which is the limit of the current computer model. Note that the SeaScan processor is at Reef Island is capable of averaging up to 128 scans and thus the modeled performance should provide a worst-case illustration.
3. Upgraded Terma Radar: The specifications of the new Scanter 2001 transceiver and new 21' antenna were used in the third simulation, but without including the effects of the SeaScan processor. In this case, the Scanter 2001 is capable of averaging up to 3 successive scans, so this was included in the simulation. The specifications used were extracted from the Terma radar performance manual, provided by Terma – North America.
4. Upgraded Terma Radar with SeaScan: This configuration is the identical to (3) above, except the SeaScan processor has been added. The simulation has been done with 16 scans, which is the limit of the current computer model. Note that the SeaScan processor is at Reef Island is capable of averaging up to 128 scans.

The modeled probability of detection results are plotted in Figure 4-1 as a function of range from the radar. In this case, a nominal radar height of 30 metres was used for the purposes of the simulation. While this radar height may not accurately convey the actual height of the Reef Island radar, it still serves as a useful example.

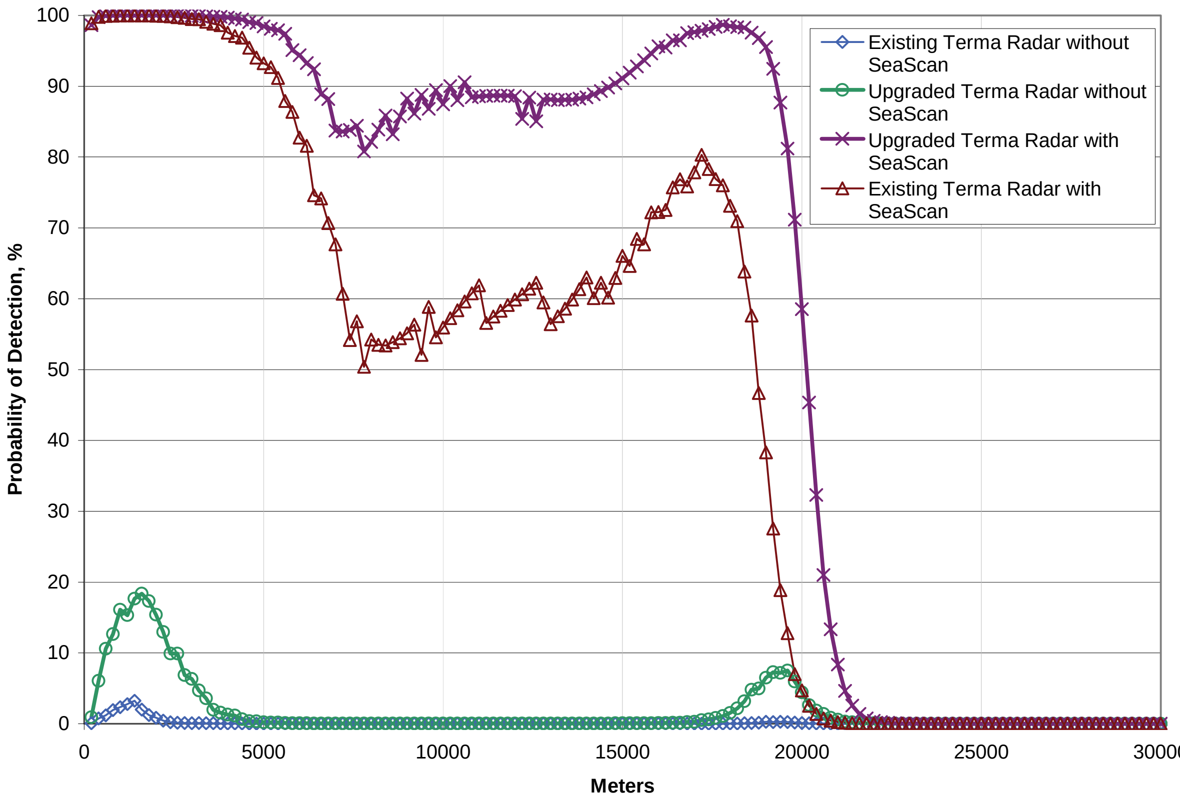

Figure 4-1. Probability of detection of a bergy bit (12m water line length) in 6 ft seas and 18 Knots wind speed with four different radar configurations.

The plot above shows a very important trend — that the probability of detection increases substantially with the addition of the SeaScan processor. For this specific example, both the existing and upgraded Terma radars have a very low probability of detection; under these circumstances, with POD less than 20%, the iceberg can be considered not detectable by that radar. However, with the SeaScan processor, the iceberg is detectable greater than 50% of the time over the detectable radar horizon. In the case of the upgraded Terma radar, the detection increase to a minimum of 80% probability of detection and more than 90% probability of detection over at least half of the range extent of the radar. This example confirms the importance of using the SeaScan processor and highlights the potential enhancement of upgrading the Reef Island system to the new Scanter 2001 transceiver and antenna.

5 RECOMMENDATIONS FOR FUTURE USE OF THE REEF ISLAND RADAR

Based on the information detailed in this report, the following recommendations are made:

1. The Reef Island radar site offers considerable advantage for mapping icebergs in Prince William Sound compared with the existing Potato Point and Spit site radars. It is recommended that Reef Island be maintained as a radar site for mapping icebergs for the foreseeable future.

2. The new Terma Scanter 2001 transceiver and 21' antenna offers an advantage over the existing Terma radar on Reef Island. The larger antenna is expected to provide enhanced target detection capabilities and the new Terma model is expected to have lower maintenance costs since it is a new unit. It is thus recommended that funding be made available for the purchase and installation of a new Terma system for Reef Island. Given the lengthy timeline suggested by the USCG for upgrading Reef Island (at least three years), it is recommended that RCAC seek their own funding for this, based on information provided by the USCG on the costs of the upgrade.

3. The new Terma Scanter 2001 transceiver is compatible with the existing SeaScan processor and thus the existing SeaScan can be interfaced with the new Terma, if this new radar were installed at some future date.

4. The SeaScan processor, combined with the new Terma radar, has significant advantage for the detection of ice compared with the existing Reef Island installation or a new Reef Island installation of a Terma Scanter 2001 alone. The scan-to-scan feature (up to 128 scans) of the SeaScan processor, combined with the 12-bit analog to digital conversion, offer significant advantages for processing iceberg targets. It is thus recommended that the SeaScan processor be maintained at Reef Island with the existing Terma radar or a future new installation of a Scanter 2001 system.

5. Given the existing communications bandwidth limitations at Reef Island, the installation of a new Terma radar would require the installation of a third party RDP to compress the radar signal to one that could be transmitted over the SERVS communications systems. Third party RDPs, like the existing LM processor, are not configured for the detection of ice. Instead, the RDPs convert the radar signal to a low dynamic range display with a 3 Hz refresh rate. Since this type of radar signal is necessary for VTS applications, it is recommended that a SeaScan display be maintained at Reef Island, specifically to be used for

iceberg detection. By maintaining the SeaScan processor at Reef Island, two displays can be maintained at SERVS and USGC, one which is configured for iceberg detection and one that is configured for VTS purposes. Each display can be configured for different detection criteria, and would thus have a significant advantage for maintaining safe tanker operations in the sound compared to a single radar display.

6. There SeaScan processor has a target tracking feature that is currently not used at SERVS. When the SeaScan processor was first installed, the use of the target tracking feature was investigated. However, the sheer number of icebergs in PWS led to a very cluttered display of iceberg tracks, making it unusable for the purposes of tanker navigation. However, this feature could be used for R&D purposes to determine iceberg characteristics (speeds, surface currents, etc.). Since these features are unsuitable for use in the SERVS duty office, it is recommended that a separate SeaScan display be incorporated into RCAC offices for the collection and distribution of iceberg detections and tracks. This would have the ancillary benefit of allowing RCAC personnel to have their own iceberg map of the Sound.

7. The SeaScan display computer at SERVS was equipped with a feature to email a screen-grab of the SeaScan processor to a select distribution list. This feature appears to be underutilized. It is recommended that the features of this email system be discussed at a future meeting between SERVS, RCAC and USCG to determine if this feature should be enabled. This feature could eliminate the need for additional displays to be installed at USCG or RCAC since the system essentially provides a complete picture of the radar display as an email attachment. In the case of RCAC, this system does not eliminate the need of a separate display for iceberg tracks, if this tracking feature is to be exploited in the future.

6 APPENDIX A - ICEBERG DETECTION USING THE SEASCAN RADAR PROCESSOR

6.1 Background

In the summer of 1999 a quantitative detection evaluation study was undertaken to assess the iceberg detection capability of the SeaScan radar processor system. In order to effectively integrate the SeaScan system with an Ice Management System it is necessary to quantify how well the system works for iceberg detection. With this as its objective, a field evaluation program was conducted in the summer of 1999 at Twillingate, Newfoundland. This site was selected as it was expected to provide sufficient iceberg targets for an effective evaluation of the system.

A Raytheon Pathfinder MK2 X-band radar with 7 foot antenna on loan from Raytheon Marine was used for the trial. This radar is the same model used on the Terra Nova FPSO with the exception that the FPSO has a 12 foot X-band antenna. The 12 foot antenna will provide better performance over the 7 foot antenna due to its better resolution and higher gain.

In order to facilitate evaluation of the SeaScan system it was equipped with recording capability for the trial. This would permit both in field evaluation and post field trial evaluation of the system. This is possible as the data recording capability provides full bandwidth raw radar data. This capability enables the re-creation of the exact situation as it occurred in the field and to try different processing and tracking parameters.

During the two week evaluation period data was collected on over 69 icebergs in a range of environmental conditions. Iceberg ground truth data was collected by C-CORE and this data was used to identify targets for detection analysis. Twenty data tapes of data were collected representing 200 Gbytes of raw radar data. Wind varied from light to a maximum of 64 kph (36 kts). Numerous rain events occurred where a rain front moved in over iceberg targets. The maximum estimated wave height was 3 meters, occurring during a 50 to 64 kph wind.

6.2 Introduction

The results of the data analysis of the 1999 field trial were reported earlier and demonstrated the capabilities of the SeaScan processor in enhancing iceberg detection. The data collected provides for specific cases of detection; however, in practice these results cannot directly be used to predict the effectiveness of Ice Management Operations as they are too specific and the inherent variability of icebergs and environmental conditions may make individual cases unrepresentative of average performance. A more useful approach is to use measured detection results to compare with modeled radar performance. The validated model may then be used to predict detection capability under a range of environmental and for a selection of icebergs.

During the period 1989 to 1991 Sigma Engineering Limited developed a model for predicting iceberg detection capability of microwave radar. The model was developed using electromagnetic wave theory and radar data collected from field trials conducted offshore Newfoundland from 1984 to 1987. The model has been used in various studies over the past ten years to predict iceberg detection. The model is also capable of simulating the effect of radar signal processing as implemented in the SeaScan processor so it is possible to use the model to predict how well the SeaScan processor will perform in iceberg detection.

Other than the early validation work that was conducted when the model was first developed there has not been a quantitative comparison of actual detection versus predicted detection, particularly when using the SeaScan processor. The data collected at Twillingate in 1999 provides a good opportunity to test the model's capability to predict SeaScan detection performance.

The following report provides the results of a quantitative comparison of actual detection performance versus predicted detection performance.

6.3 Methodology

Target detection performance is measured in terms of Probability of Detection (P_d) and Probability of False Alarm (P_{fa}). This means for a given set of operational conditions and display and processor settings a target will be visible or detected a percentage of the time and there will be a corresponding number of false alarms caused by system noise and clutter from sea and rain echos. There is a trade off in these two quantities. The higher the number of false alarms (higher P_{fa}) displayed, the higher the probability of detection(P_d) will be. In order to achieve optimal detection performance a radar operator will normally set up the radar display and adjusts the radar processing to display a small number of false alarms. This is similar to automatic detection systems where the tracker can tolerate and reject a small number of false alarms. If the system is setup so that there are no false alarms then it is likely that detection performance will not be as good as possible particularly for small targets such as icebergs in sea clutter.

The radar performance prediction model uses the radar parameters and prevailing environmental conditions to predict probability of detection as a function of range for a given probability of false alarm. Under typical operating conditions a probability of false alarm in the range of 10^{-6}

to 10^{-4} is used. This means that in one radar scan 1 to 100 false alarms will be displayed. A trained operator or sophisticated target tracker can tolerate this false alarm rate.

The Twillingate data was reviewed and targets that had the best ground truth information were selected for detection analysis. Data analysis software was used to automatically compute the target detection probability for the selected target and the false alarm probability for a region close to the targets position.

For each iceberg analyzed, a target detection window was setup and nearby a window for computing false alarms was setup. Figure 5-1 illustrates the windows setup to analyze detection of a bergy bit. The software processes a large number of radar scans and generates P_d and P_{fa} as the detection threshold is changed.

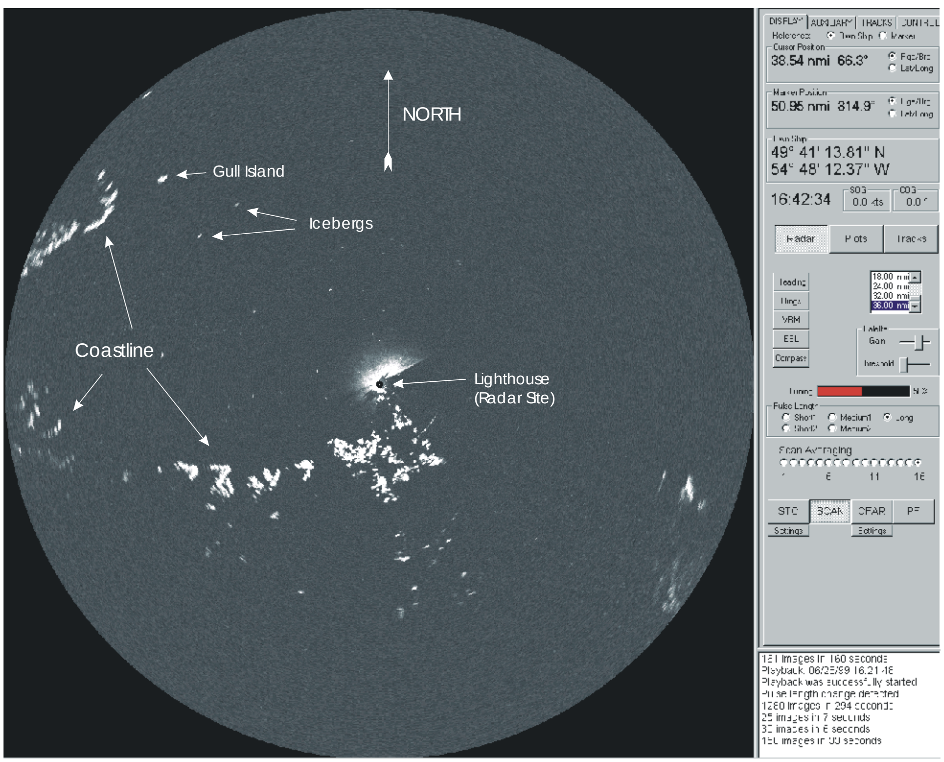

Figure 6-1. SeaScan Display showing overview of area

The radar model is then used to compute probability of detection using the radar parameters, environmental conditions and measured P_{fa} .

6.3.1 Radar Site Characteristics

Latitude: N49° 41.230'

Longitude: W54° 48.206'

Height: 300 feet(91 meters)

Radar Horizon: 21 nmi(39 km)

6.3.2 Data Summary

The following section summarizes the data selected for analysis.

6.3.2.1 Environmental Data

Tables 5-1 and 5-2 summarize the environmental conditions during the SeaScan data collection and evaluation. Sea state information was estimated visually. Wind speed and direction were measured using an anemometer mounted close to the radar. There may be differences between the wind speed measured at the radar and the wind speed at the ocean surface. The precipitation is noted as being present and what type. Often during the data collection rain would move through the area and at any point in time was localized. This had the effect of limiting detection on some icebergs for brief periods of time as the rain moved over the iceberg.

The maximum wind speed during the trial occurred on June 26th and was 64 kph with associated waves of 3 to 4 meters.

Table 6-1. Environmental Data for SeaScan Evaluation

Date(mm/dd)	Time(local)	Wind (kph, dir)	Precipitation	Seas	Comments
06/26	09:46	20 - 25, SSW	None	<1 m	
	10:26	11 - 16, SSW	None	<1 m	
	12:14	13 - 16, SW	None	<1 m	
	12:33	11 - 14, SW	None	<1 m	
	13:15	10 - 20, WSW	None	<1 m	
	17:27	16 - 18, SSW	Yes	1 m	Rain moving in
	17:52	20 - 24, SW	Yes	1 m	Wind Gusts
	17:55	30, SW	Yes	1 to 2 m	
	17:58	31, SW	Yes	1 to 2 m	
	18:09	25 - 30, SW	Yes	1 to 2 m	
06/27	09:32	29 - 34, S	No	1 to 2 m	
	09:54	31 - 31, S	No	1 to 2 m	
	10:26	24 - 27, SSW	No	1 to 2 m	
	11:13	19 - 23, SSW	No	1 to 2 m	
	11:37	13 - 18, SW	No	1 to 2 m	
	12:01	16 - 18, SW	No	1 to 2 m	
	17:41	40 - 50, NW	No	3 to 4 m	Gusts to 64 kph
06/28	10:12	20, NNE	No	1 - 2 m	

Date(mm/dd)	Time(local)	Wind (kph, dir)	Precipitation	Seas	Comments
	10:44	16 - 18, NNE	No	1 - 2 m	
	11:45	14 - 16, NNE	No	1 - 2 m	
	12:22	12 - 16, N	No	1 - 2 m	
	14:26	4 - 8, NE	No	1 - 2 m	Haze present
	17:29	6 - 10, NE	No	1 - 2 m	
	17:49	10 - 12, SW	No	1 - 2 m	Radar Problem
	18:48	10 - 12, SW	No	1 - 2 m	Weak Signals

Table 6-2. Environmental Data for SeaScan Evaluation

Date	Time(local)	Wind (kph, dir)	Precipitation	Seas	Comments
06/29	09:07	10 - 12, E	RDF	1 m	Rain, Drizzle, Fog
	11:06	11, E	Fog	1 m	Weak Radar Signals
	17:07	14 - 18, E	No	1 m	
	17:21	21, E	No	1 m	Weak Radar Signals
06/30	12:00	25, SSE	No		Gusts to 50 kph
	14:21	13 - 14, SE			
	14:49	13 - 14, SE	Rain		
	18:00	18 - 19, SE			
07/07	14:37	11, NNE	Rain	1 to 2 m	Fixed Radar
	15:37	6, E	Misty	1 to 2 m	Boat: Wind 15kts
	17:56	16 - 20, NE	Rain	1 to 2 m	
07/08	09:06	24, SSW	No	3 m	swell
	09:21	18, SSW	No	3 m	swell
	10:59	18 - 26, SSW	No	3 m	swell
	11:23	18 - 24, SSW	No	3 m	swell
	13:52	14, SW	No	3 m	swell
	14:49	14, SW	No	3 m	Calibration
	18:07	6 - 9, SW	No	3 m	swell
07/09	09:00	19 - 23, NW	No	3 m	swell
	12:54	10 - 13, NNW	No	3 m	swell
	14:26	6 - 8, N	Rain	3 m	rain clouds
	20:42	0	Rain	3 m	rain clouds
	21:16	light	Rain	3 m	
07/10	08:23	18 - 19, S	No	2 m	Lot of small boats

6.3.2.2 Iceberg Data

Table 6-3 lists icebergs selected for detection analysis. Icebergs were selected that are representative of the range of iceberg sizes and environmental conditions of interest identified during the field trial. Where available the iceberg dimensions are given.

In Table 5-3 icebergs are identified by a Field ID which is a number if measured or identified by C-CORE or a letter if assigned by Sigma. A report ID (1st column) is assigned for ease of reference. Photographs of the icebergs are contained in the field report compiled by C-CORE.

Table 6-3. Iceberg Data Selected for Detection Analysis

ID	Date	Field ID	Length (m)	Height (m)	Description	Range (nmi)	Bearing (degrees)	Detect
R1	06/26	1	6, 12, 7, 12	4	Bergy Bit	7.3	246.0	Yes
R2		2	16, 19, 20	5	Bergy Bit	6.5	227.0	Yes
R3		3	32, 26	8	Small Wedge	5.4	218.0	Yes
R4	06/27	A	5	1	Growler	0.4	341.0	Yes
R14		9	12, 13	3	Bergy Bit	6.0	246.0	Yes
R15		10	3	1	Growler	3.0	51.2	Yes
R16		11	4	1	Growler	3.1	51.9	Yes
R17		12	3		Growler	3.2	52.7	Yes
R28		7	100, 80		Medium	30.4	325.6	Yes
R29		8	100, 50		Medium	22.5	306.3	Yes

6.4 Analysis Results

6.4.1 Bergy Bit detection, R2

Iceberg R2 was a Bergy Bit encountered on June 26th having an average length of 18 meters and height of 5 meters. The conditions were calm and clear with winds from the SouthWest at about 5 knots. Figure 5-1 shows the data collection windows used for the detection analysis. In the case of unprocessed radar data 750 consecutive radar scans were analyzed for detections and false alarms. Table 5-4 below presents the results of measured probability of detection for various detection thresholds with no radar processing applied. The radar pulse length was Medium1(250 ns). Detection was limited by system noise only.

Table 6-4. Measured Detections for Bergy Bit R2 with no radar processing

		Target Opportunities	Clutter/Noise Opportunities	Target Range
		750	705000	6.0 nmi
Threshold	Target Detections	Target Pd	Clutter/Noise Detections	False Alarm Probability
45	614	0.82	92	1e-04
47	589	0.79	12	2e-05
52	485	0.65	6	9e-06
57	405	0.54	6	9e-06
62	279	0.37	5	7e-06
67	170	0.23	1	1e-06

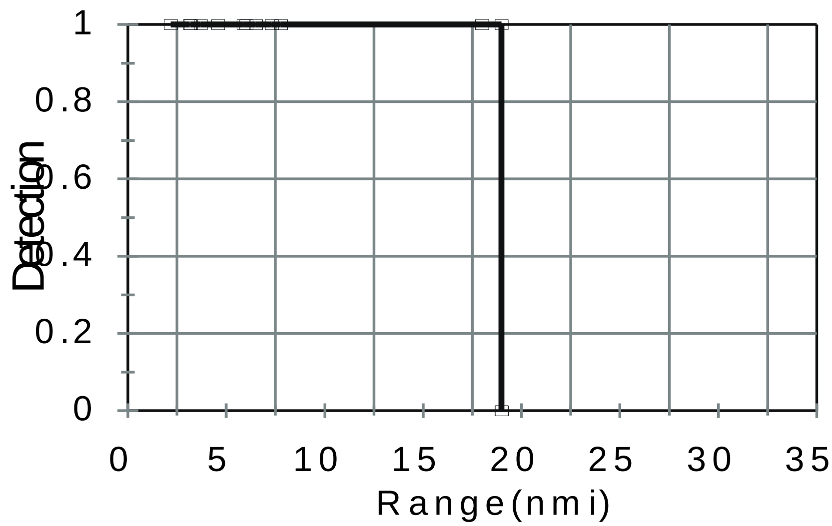

Figure 6-2. Bergy bit detections

Figure 5-2 presents a plot of Probability of Detection versus range for this Bergy Bit with the False Alarm Probability set to 1e-05. At the range of 6 nmi the modeled probability of detection is 0.62 and this agrees well with the measured detection for thresholds of 52 and 57 which provide the closest measured False Alarm Probability to 1e-05. This bergy bit was easily detectable at this range without additional radar processing.

Table 6-5. Measured Detections for Bergy Bit R2 with full radar processing

		Target Opportunities	Clutter Opportunities	Target Range
		600	600000	6.0 nmi
Threshold	Target Detections	Target Pd	Clutter Detections	False Alarm Probability
24	600	1.00	0	0e+00
25	600	1.00	0	0e+00
26	600	1.00	0	0e+00
27	600	1.00	0	0e+00

After full radar processing was applied the probability of detection was raised to 1 with no measurable false alarms (Table 5-5).

The model was used to compute the Probability of Detection versus range for this Bergy Bit with the False Alarm Probability set to a lower value of 1e-06 and full processing applied. At the range of 6 nmi the model computed probability of detection is 1.0 and this agrees well with the measured detection.

6.4.2 *Small Iceberg Detection, R3*

Iceberg R3 was a Small wedge shaped iceberg encountered on June 26th having an average length of 29 meters and height of 8 meters. The conditions were calm and clear with winds from the SouthWest at about 5 knots. In the case of unprocessed radar data 600 consecutive radar scans were analyzed for detections and false alarms. Table 5-6 below presents the results of measured probability of detection for various detection thresholds with no radar processing applied. The radar pulse length was Medium1 (250 ns). Detection was limited by system noise only.

Table 6-6. Measured Detections for Small Iceberg R3 with no radar processing

		Target Opportunities	Clutter/Noise Opportunities	Target Range
		600	662400	5.7 nmi
Threshold	Target Detections	Target Pd	Clutter/Noise Detections	False Alarm Probability
45	411	0.69	10	2e-05
50	320	0.53	6	9e-06
55	235	0.39	4	6e-06
60	155	0.26	2	3e-06
65	93	0.16	2	3e-06

Figure 5-3 presents a plot of Probability of Detection versus range for this Small Iceberg with the False Alarm Probability set to 1e-5. At the range of 6 nmi the modeled probability of detection is 0.80 and this is greater than the marginal detection observed in the measured data. Upon review of the photographs of this iceberg it is clear that the wedge shape could significantly reduce the radar cross section below that predicted by the model which assumes an average shape that is like a blocky iceberg. In this case the model overestimates the detection probability.

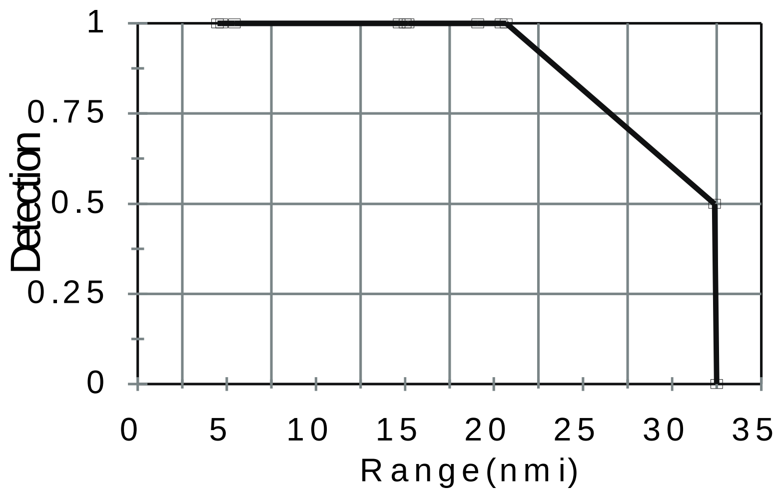

Figure 6-3. Small iceberg detections

Table 6-7. Measured Detections for Small Iceberg R3 with full radar processing

		Target Opportunities	Clutter Opportunities	Target Range
		600	662400	5.7 nmi
Threshold	Target Detections	Target Pd	Clutter Detections	False Alarm Probability
25	600	1.00	0	0e+00

After full radar processing was applied, the probability of detection was raised to 1.0 with no measurable false alarms (Table 5-7).

The model was used to compute the Probability of Detection versus range for this Iceberg with the False Alarm Probability set to a lower value of 1e-06. At the range of 6 nmi the model computed probability of detection is 1.0 and this agrees well with the measured detection.

6.4.3 Small Iceberg Detection In Rain , R3

Later in the day on June 26th rain moved through the study area and an opportunity to collect data for Iceberg R3 during a rain squall occurred. The Small Wedge shaped iceberg was 3.8 nmi from the radar when a rain squall moved over it. The average length of the iceberg was 29 meters and a height of 8 meters. The rain was brief but heavy and was probably in the range of 8 to 16 mm/hr. The radar pulse length was Medium1 (250 ns). Detection was limited by rain clutter.

Six Hundred radar scans were analyzed covering the period before the rain, during and after the rain. With full radar processing applied there was a complete loss of detection for a period of 70 seconds covering scans 186 to 214. Before and after this the iceberg was 100% detectable.

Figure 5-4 presents a plot of Probability of Detection versus range for this Small Iceberg in 8 mm/h rain with the False Alarm Probability set to 1e-6. At the range of 3.8 nmi the modeled probability of detection is 0.40 for 8 mm/hr rain. Figure 5-5 presents results for 16 mm/h rain and the modeled probability of detection is 0.02 in this case. The intensity of the rain squall was probably closer to the 16 mm/hr rate at its peak and this predicted detection agrees with the measured loss in delectability during this period.

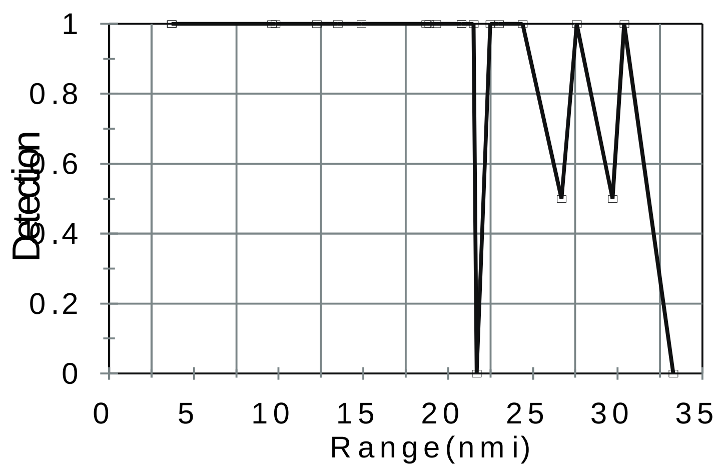

Figure 6-4. Medium iceberg detections

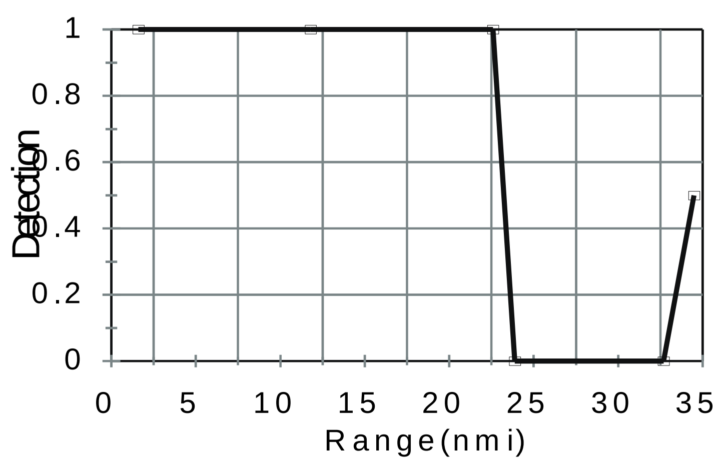

Figure 6-5. Large iceberg detection

6.4.4 Growler detection, R4

Iceberg R4 was a growler encountered early on June 27th. The wind was 15 to 17 knots (29 to 34 km/h) from the South with waves in the range of 1 to 2 meters. Figure 5-6 shows the data collection windows used for the detection analysis. In the case of unprocessed radar data 200 consecutive radar scans were analyzed for detections and false alarms. Table 5-8 presents the results of measured probability of detection for various detection thresholds with no radar processing applied. The radar pulse length was Short (60 ns). The iceberg was not detectable without radar processing. Detection was limited by sea clutter.

Table 6-8. Measured Detections for Growler R4 with no radar processing

		Target Opportunities	Clutter/Noise Opportunities	Target Range
		200	216000	0.45 nmi
Threshold	Target Detections	Target Pd	Clutter/Noise Detections	False Alarm Probability
75	26	0.13	14	6e-05
80	18	0.09	2	9e-06
85	7	0.04	1	5e-06

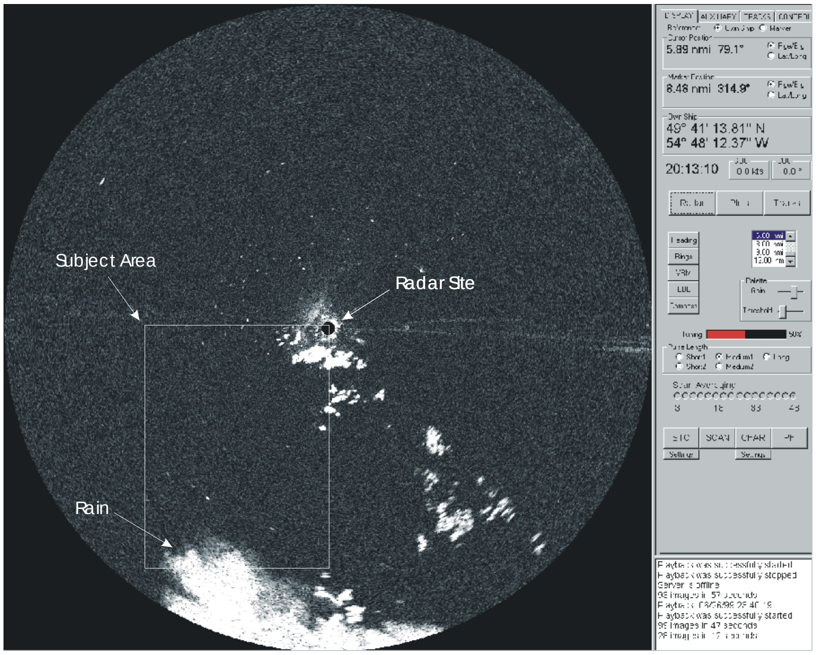

Figure 6-6. Overview of approaching rain and subject area

Figure 5-7 presents a plot of Probability of Detection versus range for this Growler with the False Alarm Probability set to 1e-05. At the range of 0.45 nmi the modeled probability of detection is 0.05 and this agrees reasonably well with the measured detection for threshold of 80. This Growler was not detectable at this range without additional radar processing.

Table 6-9. Measured Detections for Growler R4 with full radar processing

		Target Opportunities	Clutter Opportunities	Target Range
		200	216000	0.45 nmi
Threshold	Target Detections	Target Pd	Clutter Detections	False Alarm Probability
40	200	1.00	4	2e-05

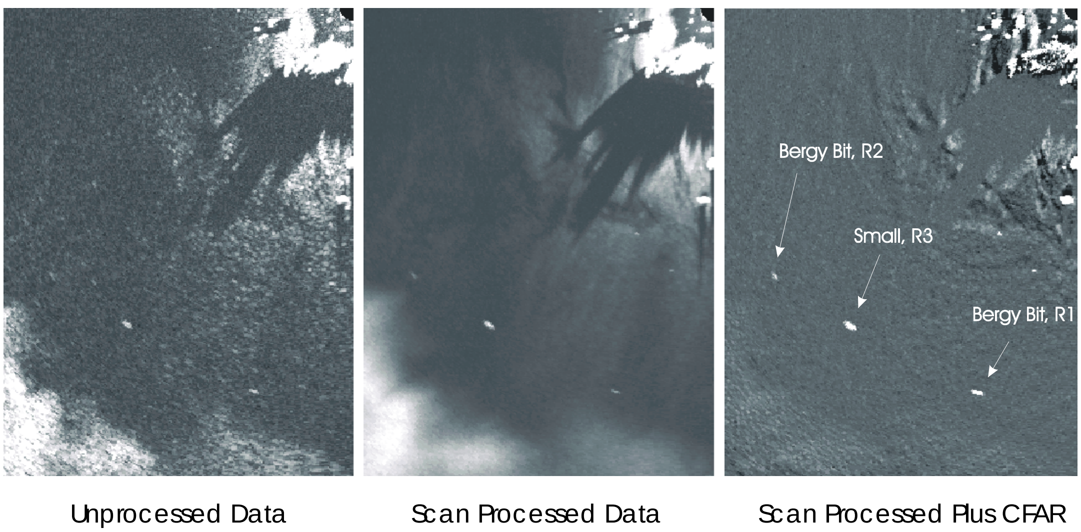

Figure 6-7. Rain approaching three icebergs

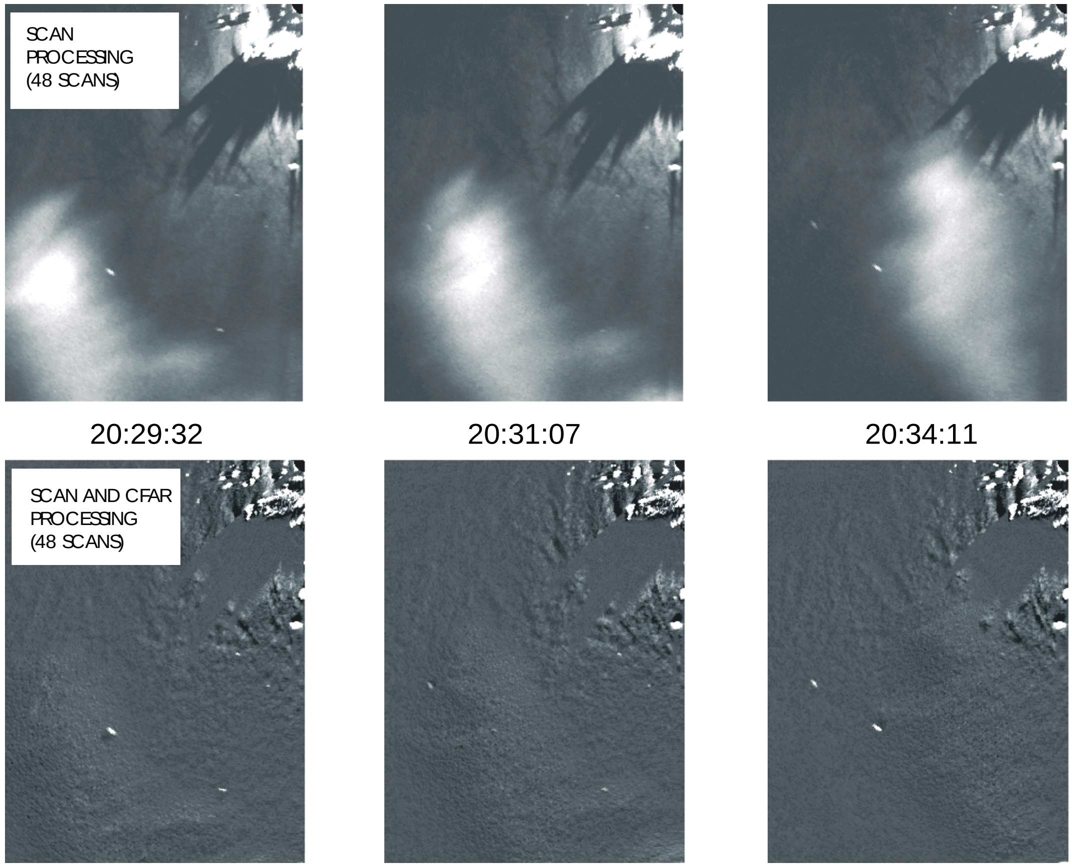

Figure 6-8. Rain moving over icebergs

After full radar processing was applied the probability of detection was raised to 1 with probability of false alarm 2e-5 (Table 5-9). In this case only 12 radar scans were averaged during the radar processing as the growler was traveling at a speed of 1 knot.

The model was used to compute the Probability of Detection versus range for this Growler with the False Alarm Probability set to 1e-05 and results are presented in Figure 5-8. At the range of 0.45 nmi the model computed probability of detection is 1.0 and this agrees well with the measured detection.

6.4.5 Bergy Bit Detection, R14

Iceberg R14 was a Bergy Bit encountered on June 27th having a length of 13 meters and a height of 3 meters. Winds were from the SSW at 12 to 14 knots (24 to 27 km/h) and seas were 1 to 2 meters. In the case of unprocessed radar data 750 consecutive radar scans were analyzed for detections and false alarms. Table 5-10 presents the results of measured probability of detection for various detection thresholds with no radar processing applied. The radar pulse length was Medium1(250 ns). Detection was limited by system noise only.

Table 6-10. Measured Detections for medium Iceberg R29 with no radar processing

		Target Opportunities	Clutter/Noise Opportunities	Target Range
		200	99000	6.0 nmi
Threshold	Target Detections	Target Pd	Clutter/Noise Detections	False Alarm Probability
38	157	0.79	21	2e-04
42	109	0.55	9	9e-05
46	78	0.39	4	4e-05
50	41	.21	3	3e-05

Figure 5-9 presents a plot of Probability of Detection versus range for this Bergy Bit with the False Alarm Probability set to 1e-05. At the range of 6 nmi the modeled probability of detection is 0.26 and this agrees reasonably well with the measured detection for thresholds of 50 which provides the closest measured False Alarm Probability to 1e-05. This bergy bit was marginally detectable at this range without additional radar processing.

Table 6-11. Measured Detections for Bergy Bit R14 with full radar processing

		Target Opportunities	Clutter Opportunities	Target Range
		200	99000	6.0 nmi
Threshold	Target Detections	Target Pd	Clutter Detections	False Alarm Probability
23	200	1.00	4	4e-05
24	200	1.00	0	0e+00
26	200	1.00	0	0e+00

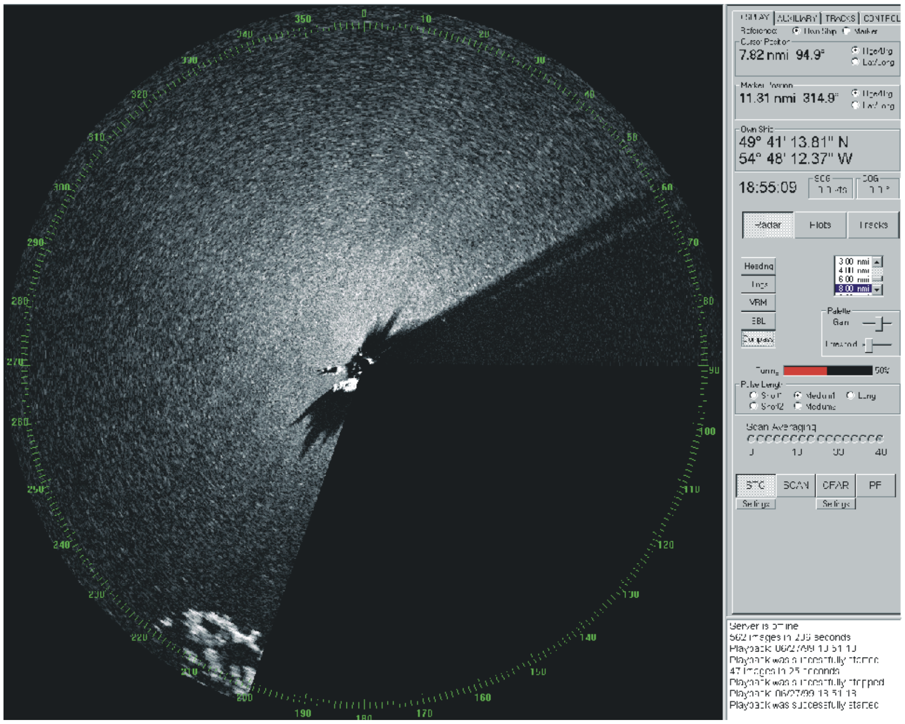

Figure 6-9. Icebergs in sea clutter – unprocessed data

After full radar processing was applied the probability of detection was raised to 1 with no measurable false alarms for detection thresholds of 24 and 26 (Table 5-11).

The model was used to compute the Probability of Detection versus range for this Bergy Bit with the False Alarm Probability set to a lower value of 1e-06. At the range of 6 nmi the model computed probability of detection is 1.0 and this agrees well with the measured detection.

6.4.6 *Bergy Bit Detection in High Sea Clutter, R14*

6.4.6.1 Short Pulse Data

Iceberg R14 was a Bergy Bit encountered on June 27th having a length of 13 meters and a height of 3 meters. In the morning on the 27th, data on this iceberg was collected under calm conditions as presented in the previous section. Later the same day the wind and waves increased significantly and another data set was collected on this iceberg. In this case the wind was from the East at 23 to 25 knots (45 to 50 km/h) with gusts to 32 knots and seas were 3 to 4 meters. In the case of unprocessed radar data 300 consecutive radar scans were analyzed for detections and false alarms. Table 5-12 presents the results of measured probability of detection for various detection thresholds with no radar processing applied. The radar pulse length in this case was Short(60 ns). Detection was limited by sea clutter.

Table 6-12. Measured Detections for Bergy Bit R14 with no radar processing

		Target Opportunities	Clutter/Noise Opportunities	Target Range
		300	234000	0.85 nmi
Threshold	Target Detections	Target Pd	Clutter/Noise Detections	False Alarm Probability
75	149	0.50	64	3e-04
80	64	0.21	18	8e-05
85	41	0.14	3	1e-05

Figure 5-10 presents a plot of Probability of Detection versus range for this Bergy Bit with the False Alarm Probability set to 1e-04. At the range of 0.85 nmi the modeled probability of detection is 0.26 and this agrees with the measured detection for thresholds of 80 which provides the closest measured False Alarm Probability to 1e-04.

Figure 5-11 presents a plot of Probability of Detection versus range for this Bergy Bit with the False Alarm Probability set to 1e-05. At the range of 0.85 nmi the modeled probability of detection is 0.04 and this is lower than the measured detection of 0.14 for a threshold of 85.

Table 6-13. Measured Detections for Bergy Bit R14 with full radar processing

		Target Opportunities	Clutter Opportunities	Target Range
		300	234000	0.85 nmi
Threshold	Target Detections	Target Pd	Clutter Detections	False Alarm Probability
42	300	1.00	0	0e+00
45	300	1.00	0	0e+00

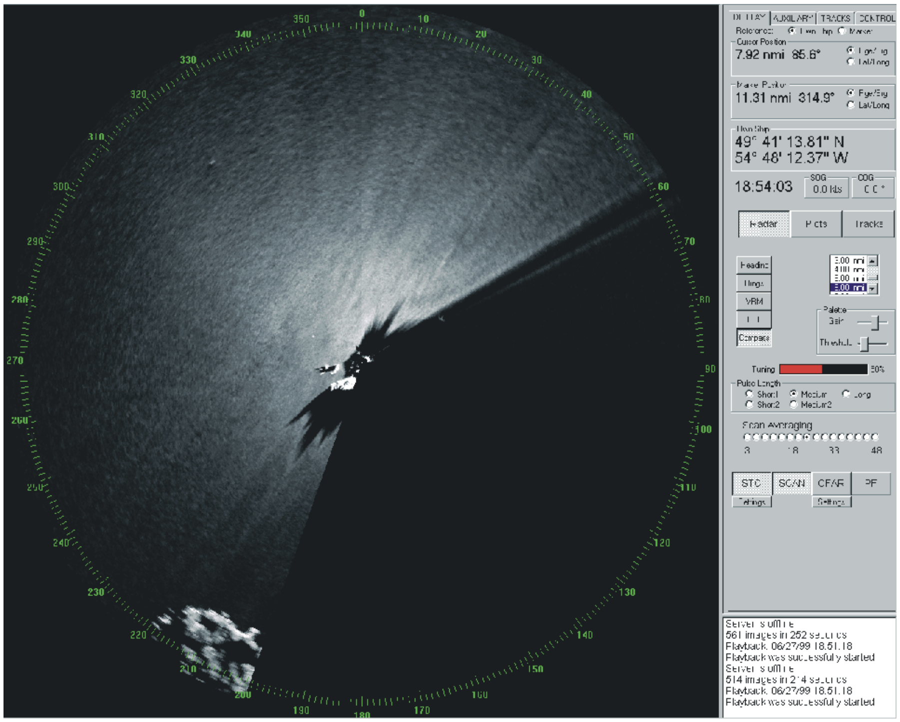

Figure 6-10. Two icebergs in sea clutter, 24 scans processed.

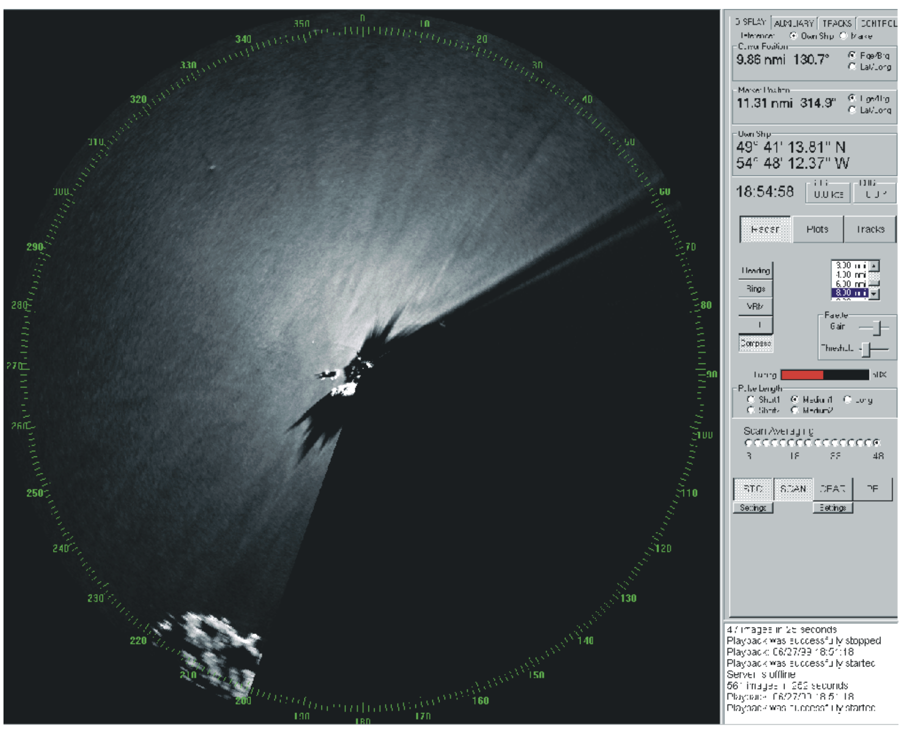

Figure 6-11. Two icebergs in sea clutter – 48 scans processed.

After full radar processing was applied the probability of detection was raised to 1 with no measurable false alarms for detection thresholds of 42 and 45 (Table 5-13).

The model was used to compute the Probability of Detection versus range for this Bergy Bit with the False Alarm Probability set to a lower value of 1e-06. At the range of 0.85 nmi the model computed probability of detection is 1.0 and this agrees well with the measured detection.

6.4.6.2 Medium Pulse Data

Iceberg R14 was a Bergy Bit encountered on June 27th having a length of 13 meters and a height of 3 meters. In the morning on the 27th data on this iceberg was collected under calm conditions as presented in the previous section. Later the same day the wind and waves increased significantly and another data set was collected on this iceberg. In this case the wind was from the East at 23 to 25 knots (45 to 50 km/h) with gusts to 32 knots and seas were 3 to 4 meters. In the case of unprocessed radar data 300 consecutive radar scans were analyzed for detections and false alarms. Table 5-14 presents the results of measured probability of detection for various detection thresholds with no radar processing applied. The radar pulse length in this case was Medium(250 ns). Detection was limited by sea clutter.

Table 6-14. Measured Detections for Bergy Bit R14 with no radar processing

		Target Opportunities	Clutter/Noise Opportunities	Target Range
		100	90000	0.85 nmi
Threshold	Target Detections	Target Pd	Clutter/Noise Detections	False Alarm Probability
64	36	0.36	3	3e-05
67	26	0.26	2	2e-05
70	20	0.20	1	1e-05
74	10	0.10	1	1e-05
76	5	0.05	0	0e+00

Figure 5-12 presents a plot of Probability of Detection versus range for this Bergy Bit with the False Alarm Probability set to 1e-05. At the range of 0.85 nmi the modeled probability of detection is 0.01and this is less than the measured detection for thresholds of 70 and 74 which provide a measured False Alarm Probability of 1e-05.

Table 6-15. Measured Detections for Bergy Bit R14 with full radar processing

		Target Opportunities	Clutter Opportunities	Target Range
		100	90000	0.85 nmi
Threshold	Target Detections	Target Pd	Clutter Detections	False Alarm Probability
33	101	1.01	4	4e-05
34	100	1.00	0	0e+00

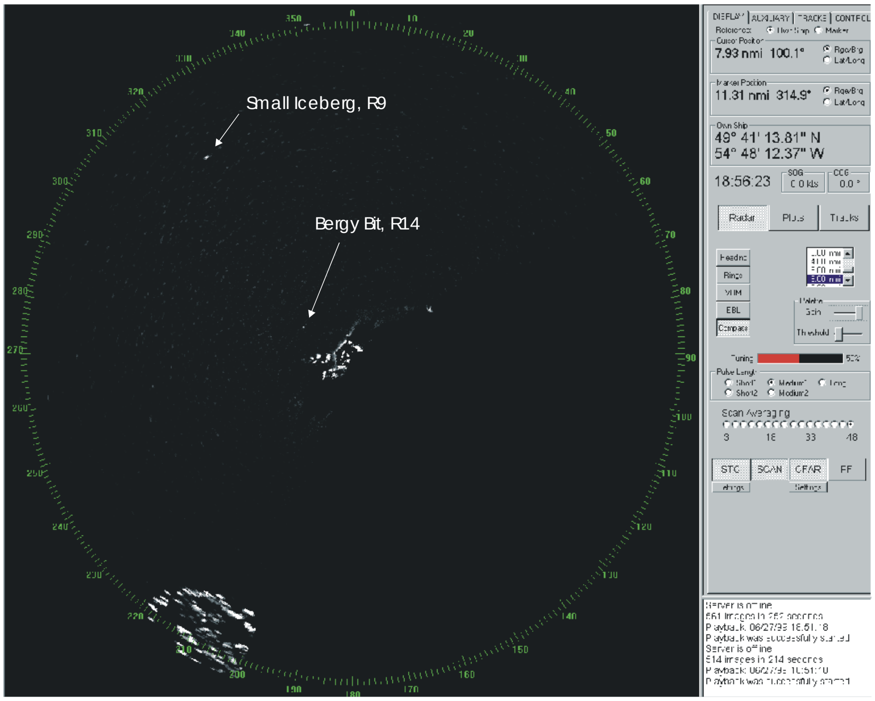

Figure 6-12. Three icebergs in sea clutter - 48 scans processed with CFAR

After full radar processing was applied the probability of detection was raised to 1 with no measurable false alarms for a detection threshold 34 (Table 5-15).

The model was used to compute the Probability of Detection versus range for this Bergy Bit with the False Alarm Probability set to a lower value of 1e-05. At the range of 0.85 nmi the model computed probability of detection is 0.92 and this agrees fairly well with the measured detection.

6.4.7 Growler Detection, R15, R16, R17

Icebergs R15, R16 and R17 were growlers encountered on June 27th. These icebergs were all approximately the same size and at the same range in a cluster. This offered the opportunity to analyze the three targets together as a group. The wind was light at 6 to 8 knots and waves were in the range of 1 meter. In the case of unprocessed radar data 200 consecutive radar scans were analyzed for detections and false alarms. Table 5-16 presents the results of measured probability of detection for various detection thresholds with no radar processing applied. The radar pulse length was Short (60 ns). The icebergs were not detectable without radar processing. Detection was limited by system noise.

Table 6-16. Measured Detections for Three Growlers with no radar processing

		Target Opportunities	Clutter/Noise Opportunities	Target Range
		600	180000	2.6 nmi
Threshold	Target Detections	Target Pd	Clutter/Noise Detections	False Alarm Probability
51	191	0.32	4	2e-05
54	174	0.29	3	2e-05
57	147	0.25	1	6e-06

Figure 5-13 presents a plot of Probability of Detection versus range for these Growlers with the False Alarm Probability set to 1e-05. At the range of 2.6 nmi the modeled probability of detection is 0.03 and this is considerably lower than the measured detection of 0.29 for threshold of 54. It was noted during analysis that one of the growlers was consistently more detectable than the other two and this would tend to bias the results. These Growlers were not reliably detectable at this range without additional radar processing.

Table 6-17. Measured Detections for Three Growlers with full radar processing

		Target Opportunities	Clutter Opportunities	Target Range
		600	180000	2.6 nmi
Threshold	Target Detections	Target Pd	Clutter Detections	False Alarm Probability
24	611	1.02	83	5e-04
25	530	0.88	1	6e-06
26	451	0.75	0	0e+00

After full radar processing was applied the probability of detection was raised to 0.88 with probability of false alarm 6e-6(Table 5-17).

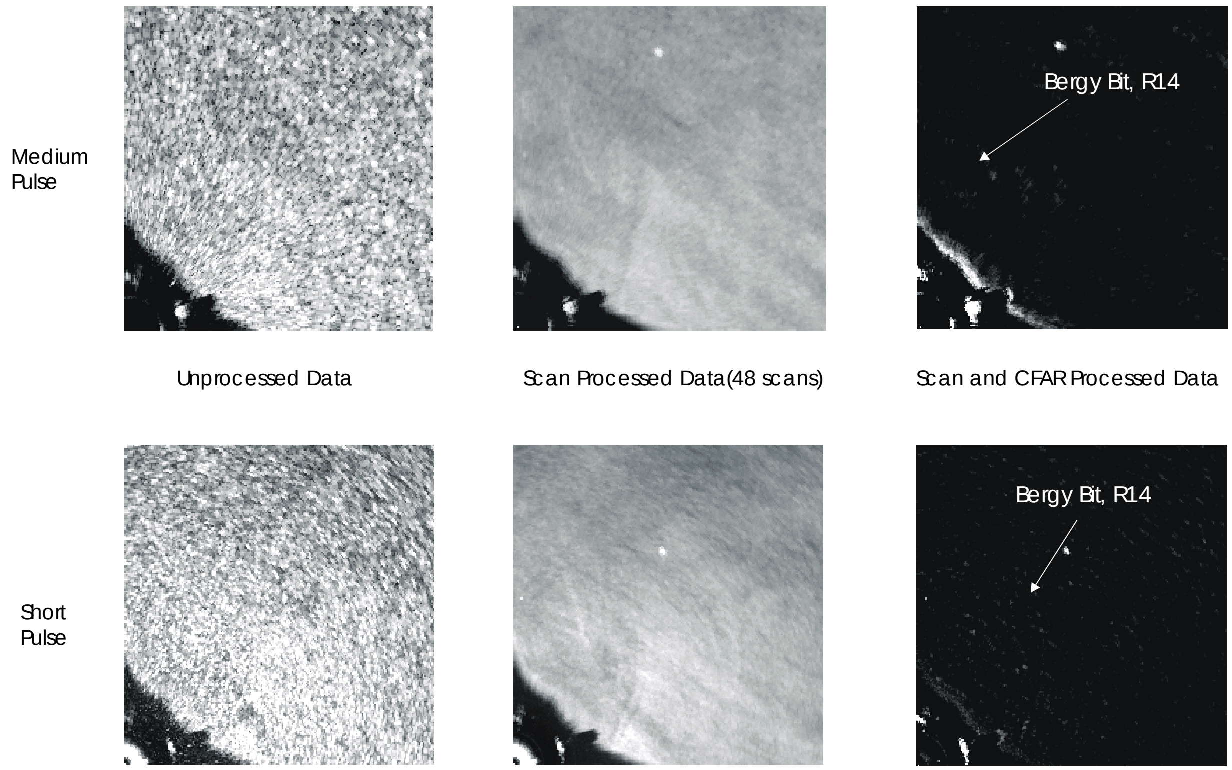

Figure 6-13. Bergy bit in sea clutter for two pulse lengths

The model was used to compute the Probability of Detection versus range for these Growlers with the False Alarm Probability set to 1e-05. At the range of 2.6 nmi the model computed probability of detection is 0.99 and this agrees reasonably well with the measured detection.

6.4.8 Medium Iceberg Detection, R28

R28 was a Medium Iceberg encountered on June 28th having a length of 100 meters and width of 80 meters. The height is estimated to be 65 meters. In the case of unprocessed radar data 300 consecutive radar scans were analyzed for detections and false alarms. Table 5-18 presents the results of measured probability of detection for various detection thresholds with no radar processing applied. The radar pulse length in this case was Long (1us). Detection was limited by noise.

Table 6-18. Measured Detections for Medium Iceberg R28 with no radar processing

		Target Opportunities	Clutter/Noise Opportunities	Target Range
		600	117000	30.5 nmi
Threshold	Target Detections	Target Pd	Clutter/Noise Detections	False Alarm Probability
42	366	0.61	148	1e-03
44	318	0.53	73	6e-04
47	256	0.43	30	3e-04
49	215	0.36	17	1e-04
52	177	0.30	9	8e-05

Figure 5-14 presents a plot of Probability of Detection versus range for this Medium Iceberg False Alarm Probability set to 1e-04. At the range of 30.5 nmi the modeled probability of detection is 0.00 and this is less than the measured detection. Note this iceberg is well over the radar horizon so observed detection must be explained by anomalous propagation conditions such as super refraction. The model does not consider this type of propagation.

Table 6-19. Measured Detections for Medium Iceberg R28 with full radar processing

		Target Opportunities	Clutter Opportunities	Target Range
		600	117000	30.5 nmi
Threshold	Target Detections	Target Pd	Clutter Detections	False Alarm Probability
27	555	0.93	7	6e-05
30	506	0.84	0	0e+00

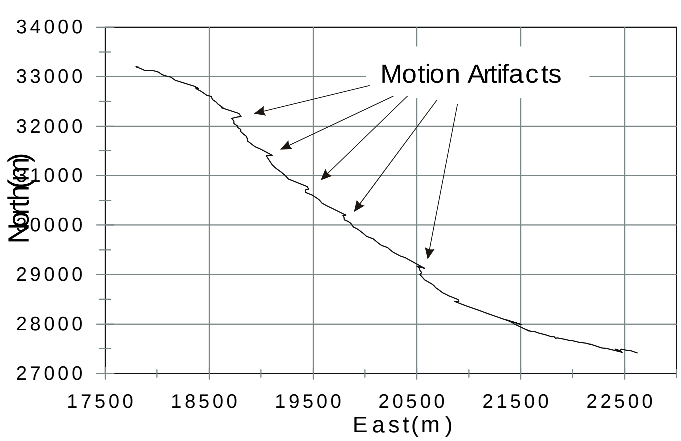

Figure 6-14. Iceberg track for a 10 hour period

After full radar processing was applied the probability of detection was raised to 0.84 with no measurable false alarms for a detection threshold 30 (Table 5-19).

The model was used to compute the Probability of Detection versus range for this Medium Iceberg with the False Alarm Probability set to a lower value of 1e-05. At the range of 30.5 nmi the model computed probability of detection is 0.00 and this is much lower than the measured detection.

6.4.9 Medium Iceberg Detection, R29

R29 was a Medium Iceberg encountered on June 28th having a length of 100 meters and width of 50 meters. The height is estimated to be 45 meters. In the case of unprocessed radar data 600 consecutive radar scans were analyzed for detections and false alarms. Table 5-20 presents the results of measured probability of detection for various detection thresholds with no radar processing applied. The radar pulse length in this case was Long(1us). Detection was limited by noise.

Table 6-20. Measured Detections for Medium Iceberg R28 with no radar processing

		Target Opportunities	Clutter/Noise Opportunities	Target Range
		600	117000	22.0 nmi
Threshold	Target Detections	Target Pd	Clutter/Noise Detections	False Alarm Probability
55	327	0.55	3	3e-05
57	290	0.48	2	2e-05
60	256	0.43	2	2e-05
62	230	0.38	2	2e-05
65	203	0.34	2	2e-05

Figure 5-15 presents a plot of Probability of Detection versus range for this Medium Iceberg False Alarm Probability set to 1e-05. At the range of 22 nmi the modeled probability of detection is 0.30 and this agrees fairly well with the measured data. Note this iceberg is at the radar horizon.

Table 6-21. Measured Detections for Medium Iceberg R29 with full radar processing

		Target Opportunities	Clutter Opportunities	Target Range
		600	117000	22 nmi
Threshold	Target Detections	Target Pd	Clutter Detections	False Alarm Probability
28	600	1.00	0	0e+00
29	600	1.00	0	0e+00
31	600	1.00	0	0e+00

After full radar processing was applied the probability of detection was raised to 1.0 with no measurable false alarms for detection thresholds of 28, 29 and 31 (Table 5-21).

The model was used to compute the Probability of Detection versus range for this Medium Iceberg with the False Alarm Probability set to a lower value of 1e-06. At the range of 22.0 nmi the model computed probability of detection is 1.00 which agrees with the measured result.

6.5 Conclusions

A quantitative analysis of iceberg detection has been carried out and results compared to detection predicted by a radar performance model. Nine icebergs were analyzed from Growler to Medium size in noise, sea and rain clutter limited detection.

In general, there is good agreement between the measured detection and the model predicted detections for all iceberg sizes. The following provides a summary of the results.

Detection of Bergy Bit R2 at a range of 6 nmi agreed very well with model predictions for both unprocessed and processed radar data.

Small Iceberg R3 at a range of 5.7 nmi was measured to have a marginal detection probability while the model predicted much better detection. Upon examination of photographs of this iceberg it was concluded that its wedge shape was probably the contributing factor in this discrepancy.

Small Iceberg R3 was also used in a detection analysis when rain is the limiting factor. Data on this iceberg was analyzed when a heavy rain squall moved over the target. During a period of 70 seconds, loss of detection occurred. This agrees well with predicted loss of detection for rain falling at 16 mm/h.

Analysis of a growler at near range (0.45 nmi) in sea clutter limited detection provided good agreement with model detection for both unprocessed and processed radar data. The growler was not detectable in unprocessed radar data and detection probability was raised to 100% after processing.

Iceberg R14 (Bergy Bit) was analyzed in a system noise limited case and good agreement was achieved for both processed and unprocessed data. Later the same day winds and seas increased and this iceberg was analyzed in a sea clutter limited situation. Short and medium pulse data were reviewed and good agreement was achieved with predicted results for short pulse on unprocessed and processed data. The model predicted a lower detection probability than the measured result for medium pulse (1% versus 10-20%) in the unprocessed case. It is expected that the short pulse detection should be better than medium pulse detection; however, in this case measured detection for the two pulses was actually the same. This may be related to different clutter statistics for the two pulses with the medium pulse being less spiky than predicted by the model. There was good agreement on medium pulse for processed data.

Three growlers (R5, R16 and R17) located 2.6 nmi from the radar were analyzed as a cluster and it was found that measured detection was better than predicted(29% versus 3%). Later examination of the data showed that one of the growlers was more detectable than the other two and that this would bias the results high.

Two medium icebergs were analyzed, one at the radar horizon and one significantly beyond the radar horizon. For the iceberg (R29) at the radar horizon (22 nmi) detection with and without radar processing showed good agreement with the model predictions. In the case of the iceberg (R28) beyond the radar horizon (30.5 nmi) measured detection was significantly better than predicted results (36% versus 0%). It is expected that this was the result of anomalous propagation conditions such as super-refraction for which the radar beam is bent around the curvature of the earth by a greater than normal atmospheric refractive index.

7 REFERENCES

C-CORE (2005), "Ice Management JIP Year 2004", C-CORE Report Number R-04-088-300 v2, November 2005.

C-CORE (2004). Ice Management JIP Year 2003, C-CORE Report Number R-03-059-226 v2, May 2004

C-CORE (2003), Integrated Ice Management R&D Initiative, 2002, Final Report No. R-02-026-110 v2, November 2003.

C-CORE, (2002). Integrated Ice Management R&D Initiative-Year 2001. C-CORE Report R-01-24-605 to Chevron, ExxonMobil, Husky, Norsk Hydro, PERD and Petro-Canada.

C-CORE,(2001). "Integrated Ice Management R&D Initiative - Year 2000." C-CORE Report R-00-C36 to Chevron, ExxonMobil, Husky, Norsk Hydro, PERD and Petro-Canada.

C-CORE (2000), "Validation of Iceberg Detection Capabilities of RADARSAT, Phase II", Proposal Number P-99-050, C-CORE, 2000.

Crocker G., B. Wright, S. Thistle, and S. Bruneau, (1998). An assessment of Current Ice Management Capabilities. Prepared by C-CORE and B. Wright and Associates Ltd. PERD/CHC Report 20-33, St. John's, Canada.

Haykin, S., Lewis, E.O., Raney, R.K., Rossiter, J.R., Remote Sensing of Sea Ice and Icebergs, John Wiley and Sons, 1994.

Harvey, M.J. and J.P. Ryan. Further Studies on the Assessment of Marine Radars for the Detection of Icebergs. June 1986, ESRF 035, 82 p.

Howell, C., Power, D., Lynch, M., Dodge, K., Vachon, P., and Staples, G., "Dual Polarization Identification of Ship and Iceberg targets – Recent Results with ENVISAT ASAR and Data Simulations of RADARSAT-2." Advanced SAR Workshop 2007, Vancouver, BC.

Howell, C., Power, D., Lynch, M., Dodge, K., Staples, G., and Robert, G., "Ship-Iceberg Discrimination Using Polarimetric SAR Data: a Quadratic Discriminant Approach." Advanced SAR Workshop 2007, Vancouver, BC.

Kline, K., J. Ryan. and G. Warbanski. 1986 The Evaluation of Two Search Radar Systems for the Detection of Small Glacial Ice Masses. Environmental Studies Research Fund Report No

McClintock, J., R. McKenna, and C. Woodworth-Lynas, May 2007. "Grand Banks Iceberg Management." PERD/CHC Report 20-84. Report prepared for PERD/CHC, National Research Council Canada, Ottawa, ON. Report prepared by AMEC Earth & Environmental, St. John's, NL, R.F. McKenna & Associates, Wakefield, QC, and PETRA International Ltd.,Cupids, NL.

Robe, R.Q., N.C. Edwards, Jr., D.L. Murphy, N. Thayer, G.L. Hover, and M.E. Kop, 1985, Evaluation of Surface Craft and Ice Target Detection Performance by the AN/APS-135 Side-Looking Airborne Radar (SLAR), Report No. CG-D-2-86, USCG Research and Development Center, Groton, CT.

Rossiter, J.R., L.D. Arsenault, E.V. Guy, D.J. Lapp, E. Wedler, B. Mercer, E. McLaren, and J. Dempsey. (1985) Assessment of Airborne Imaging Radars for the Detection of Icebergs. September 1985, ESRF 016, 320 p.

Ryan, J.P., M. Harvey and A. Kent. (1985) The Assessment of Marine Radars for the Detection of Ice and Icebergs. August 1985, ESRF 008, 127 p.

LAST PAGE OF DOCUMENT